A semi-supervised framework for diverse multiple hypothesis testing scenarios

Jack Freestone^{1*}, William Stafford Noble^{2,3}, and Uri Keich^{4*}

¹School of Mathematical and Physical Sciences, Macquarie University

²Department of Genome Sciences, University of Washington

³Paul G. Allen School of Computer Science and Engineering, University of Washington

⁴School of Mathematics and Statistics F07, University of Sydney

*Corresponding authors: jack.freestone@mq.edu.au, uri.keich@sydney.edu.au

Abstract

Standard multiple testing procedures are designed to report a list of discoveries, or suspected false null hypotheses, given the hypotheses' p-values or test scores. Recently there has been a growing interest in enhancing such procedures by combining additional information with the primary p-value or score. In line with this idea, we develop RESET (REScoring via Estimating and Training), which uses a unique data-splitting protocol that subsequently allows any semi-supervised learning approach to factor in the available side information while maintaining finite sample error rate control. Our practical implementation, RESET Ensemble, selects from an ensemble of classification algorithms so that it is compatible with a range of multiple testing scenarios without the need for the user to select the appropriate one. We apply RESET to both p-value and competition based multiple testing problems and show that RESET is (1) powerwise competitive, (2) fast compared to most tools and (3) able to uniquely achieve finite sample false discovery rate or false discovery exceedance control, depending on the user's preference.

1 Introduction

Scientists are often interested in testing many null hypotheses, $\{H_i : i = 1, ..., m\}$. Large-scale hypothesis testing is usually achieved by assigning a p-value, p_i , or a score, Z_i , to each null hypothesis. The collection of p-values, or scores, then undergoes a filtering process that rejects a subset of these null hypotheses subject to type-1 error rate control to minimize the number of misreported true null hypotheses.

The most common choice of error rate is the false discovery rate (FDR), which is defined as the expectation of the false discovery proportion (FDP) — the fraction of true null hypotheses in the reported list of rejections, or discoveries (Benjamini and Hochberg (1995)). In this case, the filtering procedure ensures that the FDR is $\leq \alpha$ where $\alpha \in (0,1)$ is a prespecified threshold. Alternatively, we might be interested in controlling false discovery exceedance (FDX), which is the upper tail probability of the FDP. The FDX is said to be controlled with threshold α at confidence $1 - \gamma$ if $\mathbb{P}(FDP > \alpha) \leq \gamma$. Evidently, such FDX control reduces the chance that the realized FDP exceeds α , which is not guaranteed by FDR control (Guo and Romano (2007); Katsevich and Ramdas (2020); Goeman et al. (2021); Li et al. (2022); Luo et al. (2023); Ebadi et al. (2023)).

Recently, researchers have focused on developing methods that leverage side information $\mathbf{x}_i \in \mathcal{X}$, which complements each p-value, or score, to better discriminate between true and false null hypotheses. These methods utilize a variety of strategies but ultimately operate with the same goal in mind: the side information is used to weight or rescore the hypotheses according to how confidently we believe that each hypothesis is a false null.

In this paper, we offer a novel approach for multiple testing with side information. The idea is to randomly split a set of suspected true nulls into two sets, where one set is used for training a semi-supervised learning model to discriminate between the true and false null hypotheses, and the other for estimating the number of false discoveries. Accordingly, we refer to our new approach as RESET—REScoring via Estimating and Training. Our method flexibly incorporates any semi-supervised approach to help distinguish between true and false null hypotheses. Moreover, it is applicable to both competition- and p-value-based multiple testing scenarios, and allows the user to choose between FDR or FDX control. We evaluate RESET in a range of simulations and real data

applications to verify that it is a competitive alternative to existing methods in terms of statistical power and speed.

2 Background: competition-based multiple testing

In competition-based multiple testing, each hypothesis H_i is associated with two scores: a test or target score, Z_i , where larger values indicate greater evidence against the null, and a decoy score, \tilde{Z}_i , a random draw from the null distribution. Each pair (Z_i, \tilde{Z}_i) is evaluated in a head-to-head competition yielding a label $L_i \in \{\pm 1\}$ that indicates which score is higher and a winning score W_i :

$$L_i := \begin{cases} +1 & Z_i > \tilde{Z}_i \\ &, \quad W_i := f(Z_i, \tilde{Z}_i), \\ -1 & Z_i < \tilde{Z}_i \end{cases}$$

where f is symmetric in its arguments and increases with the values of Z_i and \tilde{Z}_i , or with the difference between them, e.g., $f(x,y) = \max\{x,y\}$ or f(x,y) = |x-y|. Hypotheses with ties (i.e., $Z_i = \tilde{Z}_i$) are either discarded or the ties are randomly broken. We refer to a hypothesis with $L_i = 1$ as a target win or a target for short, and $L_i = -1$ as a decoy win or a decoy for short. The winning scores and labels have two properties. First, the false nulls with large Z_i will likely win their competition, resulting in a target win $(L_i = 1)$ with large W_i . Second, the true null labels are independent and equally likely to be ± 1 , independently of everything else. This is formalized in the following assumption.

Assumption 1. Let N be the indices of the true null hypotheses. Conditioned on all the scores W, and the labels of the false null hypotheses, the true null labels $\{L_i : i \in N\}$ are i.i.d. ± 1 uniform random variables.

Given Assumption 1 holds, the number of decoy wins $(L_i = -1)$ that score above a cutoff τ can be used to conservatively estimate the number of true null hypotheses with $L_i = 1$ that are also above τ . Using this strategy, we can report a list of discoveries in one of two ways.

The first and by far the more common way is to apply Selective SeqStep+ (SSS+, Algorithm A1) (Barber and Candès (2015)), which controls the FDR under Assumption 1 at a pre-

specified threshold α . Assuming the labels L are reranked according to the scores W in descending order, SSS+ reports the following list of discoveries, R_{α} :

$$R_{\alpha} := \{ i \le \tau : L_i = 1 \}, \text{ where } \tau := \max \left\{ t \in [m] : \frac{\#\{i \le t, L_i = -1\} + 1}{\#\{i \le t, L_i = 1\} \lor 1} \le \alpha \right\},$$
 (1)

where $[m] := \{1, 2, ..., m\}$. Notably, SSS+ can be adjusted to handle a more general setting when the probabilities of the positive and negative labels of the true null hypotheses are no longer uniform (Barber and Candès (2015); Lei and Fithian (2016)).

Alternatively, we can control the FDX by using, for example, FDP-stepdown (FDP-SD, Algorithm A2) (Luo et al. (2023)). FDP-SD works by first reranking the labels L according to the scores W in descending order. Next, it compares the number of decoy wins in the first i hypotheses, denoted as $D_i := \#\{L_j = -1 : j \leq i\}$, with a precomputed bound δ_i , which is determined by α and γ . The comparisons are made in a 'stepdown' fashion: we test whether $D_i \leq \delta_i$ only if $D_j \leq \delta_j$ for j < i. For small i, it is impossible for $D_i \leq \delta_i$ and so FDP-SD begins this analysis at i_0 , the smallest possible index for which $D_i \leq \delta_i$ can occur. Under Assumption 1, reporting the following list of discoveries $R_{\alpha,\gamma}$ controls the FDX:

$$R_{\alpha,\gamma} := \{ i \in [m] : i \le k_{FDP}, L_i = 1 \}, \quad k_{FDP} := \max\{ i : \prod_{j=i_0}^{i} 1_{D_j \le \delta_j} = 1 \text{ or } i = 0 \}.$$
 (2)

2.1 Extension to side information

To our knowledge, the only 'intrinsic' competition-based multiple testing procedure that uses arbitrary side information in a data-driven manner is the recent Adaptive Knockoffs (AdaKO) by Ren and Candès (2023). AdaKO is a specialization of the p-value based procedure AdaPT (Lei and Fithian (2018)) that we introduce in the next section with further details in Section C.1. By 'intrinsic', we mean that while other p-value based approaches may be modified to be used in the competition setting, Ren and Candès (2023) demonstrate they are substantially less powerful, and are not viable in this sense. Adaptive Knockoffs works by iteratively pruning \hat{S}_t , the candidate set of hypotheses at each step t, by selecting the hypothesis it deems most likely to be a true null. To do that, it fits a classification algorithm using a strict subset of information that partially masks the

data: the scores W, the side information \mathbf{x} , and the labels $(L_i)_{i \in [m] \setminus \hat{S}_t}$ of the hypotheses that were pruned up to that point, as well as $\#\{i \in \hat{S}_t : L_i = 1\}$ and $\#\{i \in \hat{S}_t : L_i = -1\}$. In their paper, Ren and Candès (2023) investigate this pruning strategy using different types of filters: a logistic regression (LR), a generalized additive model (GAM) which is the default filter in their R package, a random forest (RF), and a two-group model which is fitted using the expectation-maximization algorithm (EM) (Dempster et al. (1977)). The pruning process terminates at step τ when the estimated FDR is less than or equal to α :

$$\widehat{FDR}_{\hat{S}_{\tau}} := \frac{\#\{i \in \hat{S}_{\tau} : L_i = -1\} + 1}{\#\{i \in \hat{S}_{\tau} : L_i = 1\} \vee 1} \le \alpha.$$
(3)

The remaining positively labelled hypotheses in \hat{S}_{τ} are then reported. It was shown that, given the following natural extension of Assumption 1, Adaptive Knockoffs controls the FDR.

Assumption 2. Let N be the indices of the true null hypotheses. Conditioned on all the scores W, the side information \mathbf{x} , and the labels of the false null hypotheses, the true null labels $\{L_i : i \in N\}$ are i.i.d. ± 1 uniform random variables.

3 Background: p-value based multiple testing

Multiple testing with FDR control was popularized by the BH procedure (Benjamini and Hochberg (1995)). Since then, numerous p-value-based methods have been developed to address multiple testing in two main ways. First, many methods build on the BH framework to improve statistical power by estimating the fraction of true null hypotheses denoted as π_0 (Storey et al. (2004); Benjamini et al. (2006); Hu et al. (2010)), reweighting p-values (Genovese et al. (2006); Blanchard and Roquain (2008); Roquain and Van De Wiel (2009); Habiger (2017); Ramdas et al. (2019)), or by reordering them (Barber and Candès (2015); Lei and Fithian (2016); G'Sell et al. (2016); Li and Barber (2017)). A second approach focuses on the stricter criterion of FDX control. One example of this second direction is the stepdown procedure proposed by Guo and Romano (2007), which we will refer to as GR-SD in our later analyses.

Table 1: Summary of some popular recent p-value based multiple testing procedures that use side information.

Method	Error control	Speed
AdaPT (2018)	Finite FDR	Slow
$AdaPT_g$ (2021)	Finite FDR	Slow
$AdaPT-GMM_g$ (2021)	Finite FDR	Slow
ZAP-asymp (2022)	Asymptotic FDR	Fast
AdaFDR (2019)	Asymptotic FDX	Fast

3.1 Extension to side information

More recent works harness side information in a data-adaptive way to further boost statistical power. Such adaptive methods include Adaptive P-value Thresholding (AdaPT) and its derivatives (Lei and Fithian (2018); Chao and Fithian (2021)), Z-value Adaptive Procedures (ZAP) (Leung and Sun (2022)) and AdaFDR (Zhang et al. (2019)). Table 1 provides a qualitative summary of each method in terms of its type-1 error control, its error control guarantees, and its computational speed. ZAP-asymp and AdaPT-GMMg also have the advantage of operating directly on the test statistic instead of the corresponding p-values, which can boost power. In this paper, we will focus our comparisons based on the p-value information. Notably, none of these mentioned tools offer a fast finite type-1 error control (FDR or FDX), and as we will see, some of these methods have variable power when considering a range of simulated and real datasets. We provide a description of these methods in Section C.1.

The list of methods we examine here is incomplete. Others include Independent Hypothesis Weighting (Ignatiadis et al. (2016); Ignatiadis and Huber (2021)) and Structure Adaptive Benjamini Hochberg Algorithm (SABHA) (Li and Barber (2019)) which both adaptively weight the p-values using side information. In addition, ZAP-finite is the analogue of ZAP-asymp which offers finite sample FDR control. It uses the same principles of the AdaPT methods where each hypothesis is pruned one at a time. However, in previous simulations and real data experiments, IHW and SABHA appeared to be consistently outperformed by some of the methods in Table 1 of the main text. Because we consider the same simulations and real data experiments, we did not include those methods in our comparisons. In addition, ZAP-finite is presented as a less powerful alternative to ZAP-asymp with the computational costs of the AdaPT methods. Given our comparisons to ZAP-asymp and the AdaPT methods, we decided to exclude ZAP-finite from our comparisons.

4 Methods

RESET is designed to control the FDR or the FDX in either the competition or p-value based setting. We next describe RESET's main steps, with further details given in Algorithm A4.

4.1 RESET

1. Intrinsically, RESET's input consists of the labels, $L = (L_i)_{i=1}^m$, the winning scores, $W = (W_i)_{i=1}^m$, and side information, $\mathbf{x} = (\mathbf{x}_i)_{i=1}^m$. Hence, in the p-value setting, each p_i is first converted to a pair (L_i, W_i) in the following way:

$$L_{i} = \begin{cases} +1 & p_{i} \in [0, a) \\ -1 & p_{i} \in (b_{1}, b_{2}] \end{cases}, \quad W_{i} = \begin{cases} |\Phi^{-1}(p_{i})| & p_{i} \in [0, a) \\ |\Phi^{-1}((b_{2} - p_{i}) \cdot \frac{a}{b_{2} - b_{1}})| & p_{i} \in (b_{1}, b_{2}] \end{cases}, \tag{4}$$

where $0 < a \le b_1 < b_2 \le 1$ and $a \le 1/2$ determine the cutoff regions for defining a positive and negative label, and Φ is the standard normal CDF (the motivation for the introduction of Φ is discussed below). Hypotheses with p-values outside of $[0, a) \cup (b_1, b_2]$ are thrown out. The default is $a = b_1 = 1/2$ and $b_2 = 1$.

- 2. RESET independently and randomly assigns each winning decoy as a training decoy with probability s (we used s=1/2 throughout). The complementary set of decoy wins defines the estimating decoy set, and the set of pseudo targets is the set of all estimating decoys and target wins. The pseudo labels, \tilde{L}_i , denotes whether the ith hypothesis is a pseudo target $(\tilde{L}_i=1)$ or a training decoy $(\tilde{L}_i=-1)$.
- 3. Next, RESET applies a user-selected semi-supervised machine learning model which uses the pseudo labels, winning scores, and side information $(\tilde{L}, W, \mathbf{x})$. Note that this is a semi-supervised task because the positive pseudo labels typically contain a mixture of true and false nulls, while the negative pseudo labels are mostly comprised of null hypotheses.

The output of this step is a rescoring of the training decoys and pseudo targets, denoted as \widetilde{W} . Ideally, \widetilde{W} scores many of the false nulls among the pseudo targets higher than they were scored originally. We provide a specific framework that we developed for this crucial step in

Section 4.4.

- 4. With the training complete, the training decoys are thrown out, and the original labels L of the remaining pseudo targets, $J := \{i \in [m] : \tilde{L}_i = 1\}$, are revealed.
- 5. Using the original labels $(L_i)_{i\in J}$ and the new scores $(\widetilde{W}_i)_{i\in J}$ RESET then determines its list of discoveries by applying either
 - (a) SSS+ (Algorithm A1) at the desired level α for FDR control, or
 - (b) FDP-SD (Algorithm A2) at the desired level α and confidence parameter γ for FDX control.

The two algorithms, SSS+ and FDP-SD, require an additional parameter c. This parameter is used to define the expected ratio of the number of null targets to decoys, $\frac{c}{1-c}$. Typically, this is set to c=1/2 for an expected target-decoy ratio of 1; however, RESET uses approximately half of the decoys for training purposes (by default). Since those decoys are subsequently thrown out, this parameter needs to be adjusted. Indeed, assuming that the labels L of the true nulls are i.i.d. uniform ± 1 RVs, and s=1/2, we set the parameter to $c=c_e:=2/3$, so that the expected target-decoy ratio is $\frac{c}{1-c}=2$. More generally, if we know that for a true null $\mathbb{P}(L_i=1) \leq c_0$, then we set $c=c_e:=\frac{c_0}{1-s\cdot(1-c_0)}$. For example, in the p-value setting, $c_0=\frac{a}{a+b_2-b_1}$. This choice is made rigorous in Lemma 1.

We note that the above application of Φ^{-1} in Equation (4) is not strictly necessary for type-1 error rate control. We apply Φ^{-1} to the p-value p_i or the mirrored p-value, $(b_2 - p_i) \cdot \frac{a}{b_2 - b_1}$, because we found that doing so makes the semi-supervised learning task of Step (3) to be generally less variable and more powerful (data not shown).

Crucially, in Step (5) the training decoys are thrown out. This is important since during the training phase of Step (3), the semi-supervised machine learning model will have presumably learned to discriminate between the training decoys and the pseudo targets. Hence, true null targets will tend to score higher than the training decoys making the latter unsuitable for estimating the number of true nulls among the top scoring hypotheses.

4.2 Other related work and contributions

Recently, Marandon et al. (2024) developed a method called AdaDetect in the application of novelty detection. Given a sample of null observations (Y_1, \ldots, Y_n) with common marginal distribution P_0 , the objective is to detect which observations in a test set (X_1, \ldots, X_m) are drawn from a different marginal distribution, i.e., $X_i \not\sim P_0$. AdaDetect uses a similar strategy to that of RESET by splitting the null observations into two parts, (Y_1, \ldots, Y_k) and (Y_{k+1}, \ldots, Y_n) . The first part is used to assist in ranking the joint observations $(Y_{k+1}, \ldots, Y_n, X_1, \ldots, X_m)$ while the second part is used to construct empirical p-values (also called conformal p-values (Bates et al. (2023))) for each test set observation. Then, the BH procedure (or one of its π_0 derivatives) is applied.

The critical assumption that guarantees AdaDetect's FDR control is that the null observations (Y_1, \ldots, Y_n) and the null test set observations $(X_i : X_i \sim P_0)$ are exchangeable, conditioned on $(X_i : X_i \not\sim P_0)$. A natural question is whether a similar set of assumptions can be applied to the multiple hypothesis setting, so that an AdaDetect-like approach can be used to control the FDR. The answer is no, and we show in Section F.1 that applying AdaDetect's idea can break FDR control.

We recently developed Percolator-RESET (Freestone et al. (2025)) that combined the RE-SET approach with Percolator, a popular semi-supervised algorithm designed specifically for FDR control in peptide detection from mass spectrometry data (Käll et al. (2007)). This manuscript includes several novel contributions over Freestone et al. (2025). First, we introduce the general RESET algorithm, which is applicable to both p-value and competition-based multiple testing scenarios. Second, we also consider FDX control and provide theoretical justification of RESET's finite sample FDR or FDX control (thereby also providing the previously-missing theoretical proof of Percolator-RESET's FDR control). Third, we introduce "RESET Ensemble" as the new semi-supervised engine of RESET's Step (c). Fourth, we conduct extensive simulated and real data experiments comparing RESET Ensemble with competing methods (including a comparison of the new RESET Ensemble to Adaptive Knockoffs in the peptide detection context). Fifth, we explore FDX control with side information for peptide detection.

4.3 RESET controls the FDR or FDX

To establish RESET's control of the FDR or FDX in both the competition and p-value settings, we relax Assumption 2 so that it can be applied to the case where the true null labels are no longer necessarily uniformly or even identically distributed:

Assumption 3. Let N be the indices of the true null hypotheses. Conditioned on W, the side information \mathbf{x} , and the labels of the false null hypotheses, the true null labels $(L_i)_{i\in\mathbb{N}}$ are independent ± 1 random variables with $\mathbb{P}(L_i=1)=:c_i\leq c_0$.

We discuss the applicability of this assumption in Sections 5 and 6 where we apply RESET in both the competition and p-value settings.

RESET's FDR/FDX control hinges on the following Lemma, which essentially states that the labels L of the true null pseudo targets in Step (5) are conditionally independent ± 1 RVs—even after we sample the training decoys in Step (2) and the application of the machine learning model in Step (3).

Lemma 1. Let $\mathcal{G} := \sigma\left(W, \mathbf{x}, (L_i)_{i \notin N}, (\tilde{L}_i)_{i \in [m]}\right)$, N be the indices of the true nulls, and $J := \{i \in [m] : \tilde{L}_i = 1\}$. Then, under Assumption 3, conditioned on \mathcal{G} , $(L_i)_{i \in J \cap N}$ are independent ± 1 RVs with

$$\mathbb{P}(L_i = -1 \mid \mathcal{G}) \ge 1 - c_e,$$

where
$$c_e := \frac{c_0}{1 - s \cdot (1 - c_0)}$$
.

Proof. Note that we can express \tilde{L}_i as $\tilde{L}_i = f(L_i, B_i)$ where f is a deterministic function and B_i are Bernoulli(s) RVs that are independent given everything else. It follows from $\tilde{L}_i = f(L_i, B_i)$ and Assumption 3 that, conditioned on $\mathcal{G}_0 := \sigma(W, \mathbf{x}, (L_i)_{i \notin N})$, the pairs in $\{(L_i, \tilde{L}_i) : i \in N\}$ are independent of one another.

Moreover, from $\tilde{L}_i = f(L_i, B_i)$ and $(L_i)_{i \notin N} \in \mathcal{G}_0$ we find that these pairs are still independent conditioned on $\sigma\left(\mathcal{G}_0, (\tilde{L}_i)_{i \notin N}\right)$. This independence in turn implies that $(L_i)_{i \in N}$ are independent if we further condition on all the pseudo labels, i.e., on $\mathcal{G} = \sigma\left(\mathcal{G}_0, (\tilde{L}_i)_{i \in [m]}\right)$. Since J is fixed conditioned on \mathcal{G} , the labels $(L_i)_{i \in J \cap N}$ are independent conditioned on \mathcal{G} , establishing the first part.

It follows from Assumption 3 and the above discussion, that with $\mathcal{G}_{-i} := \sigma\left(\mathcal{G}_0, (\tilde{L}_j)_{j \neq i}\right)$ $\mathbb{P}(L_i = -1 \mid \mathcal{G}_{-i}) \geq 1 - c_0$. Consider $i \in N$ and an atom of \mathcal{G}_{-i} where $W, \mathbf{x}, (L_j)_{j \notin N}$ and $(\tilde{L}_j)_{j \neq i}$ are all fixed. Then construing the following as conditional on that atom we have

$$\mathbb{P}(L_i = -1, \tilde{L}_i = 1) = \mathbb{P}(L_i = -1) \cdot \mathbb{P}(\tilde{L}_i = 1 \mid L_i = -1)$$

$$\geq (1 - c_0) \cdot (1 - s).$$

Hence, under the same assumptions

$$\mathbb{P}(L_i = -1 \mid \tilde{L}_i = 1) = \frac{\mathbb{P}(L_i = -1, \tilde{L}_i = 1)}{P(\tilde{L}_i = 1)} \\
\geq \frac{(1 - c_0) \cdot (1 - s)}{(1 - s) \cdot \mathbb{P}(L_i = -1) + 1 \cdot \mathbb{P}(L_i = 1)} \\
= \frac{(1 - c_0) \cdot (1 - s)}{1 - s \cdot \mathbb{P}(L_i = -1)} \\
\geq \frac{(1 - c_0) \cdot (1 - s)}{1 - s \cdot (1 - c_0)} \\
= 1 - c_e.$$

Additionally, clearly

$$\mathbb{P}(L_i = -1 \mid \tilde{L}_i = -1) = 1 \ge 1 - c_e.$$

Therefore, under the same assumptions, the following holds a.s.

$$\mathbb{P}(L_i = -1 \mid \mathcal{G}) = \mathbb{P}(L_i = -1 \mid \tilde{L}_i, \mathcal{G}_{-i}) \ge 1 - c_e.$$

It is worth noting that Lemma 1 is not true for an arbitrary splitting of the decoys into the training and estimating sets, e.g., splitting the decoys into two halves of equal size. To see this, suppose that all hypotheses are true nulls, i.e., N = [m]. Then by observing the number of training decoys, we know that the number of true null decoys in J must be the same, and the labels $(L_i)_{i \in J \cap N}$ are no longer independent. We are now ready to state our two main theorems.

Theorem 1. Under Assumption 3 RESET controls the FDR at the user-specified threshold α .

Theorem 2. Under Assumption 3 RESET controls the FDX at the user-specified threshold α and confidence $1 - \gamma$.

The proofs of Theorem 1 and 2 follow from Lemma 1 and rely on a technical discussion when the labels $(L_i)_{i\in J\cap N}$, conditioned on \mathcal{G} , are non-identical, which we give in Section B.1. To briefly see the connection of Lemma 1 to Theorems 1 and 2, note that the labels $(L_i)_{i\in J\cap N}$ are independent ± 1 RVs even after observing the machine learning scores \widetilde{W} in Step (3) and the false null labels $(L_i)_{i\notin N}$. If the labels are identical, i.e., $\mathbb{P}(L_i = -1 \mid \mathcal{G}) = 1 - c_e$, then the assumptions of SSS+ in Barber and Candès (2015) and FDP-SD in Luo et al. (2023) are satisfied, and RESET controls the FDR or FDX, respectively. Intuitively, in the non-identical case, i.e., $\mathbb{P}(L_i = -1 \mid \mathcal{G}) \geq 1 - c_e$, FDR or FDX control should be more conservative using these procedures.

4.4 Semi-supervised approach

In this section we describe our specific framework for RESET's Step (3), which can use any semisupervised machine learning model. It consists of two main steps: (1) we apply a range of classification algorithms to estimate a high quality positive set from the data, presumably containing many false nulls, and (2) this positive set is then subsequently used for a second application of the classification algorithms to rescore the hypotheses. In Section C.2, we outline some additional heuristics that we employ to improve the procedure's speed and power, as well as its applicability to dependent data.

- (i) We first define the negative and positive sets, as well as the features that are subsequently used by a collection of classification algorithms: the negative set is the set of all training decoys, the positive set is a subset of top scoring pseudo targets (Section C.2.3), and the features are the combined score and side information (W, \mathbf{x}) .
- (ii) We randomly split all the hypotheses into K folds (we used K = 3 throughout). For each considered classification algorithm, and for each $k \in [K]$, we train the classification algorithm using the features of the hypotheses in the subsets of the positive and negative sets that are

in the $[K] \setminus \{k\}$ training folds, and then we apply the trained model to all the hypotheses in the kth test fold. We consider a random forest (RF), a generalized additive model (GAM), and a collection of two-layer neural networks (NN) with decay parameter $\lambda \in \{0, 0.1, 1\}$ and a number of hidden layer nodes $h \in \{2, 5, 10\}$.

- (iii) To reduce variability, we repeat Step (ii) r times (we used r = 10).
- (iv) To evaluate each classification algorithm, we apply Selective SeqStep (SSS) (Algorithm A1, which is similar to SSS+ of Equation (1) but without the '+1') at an FDR threshold α to each of the rK test folds, using the scores obtained from the classification algorithm and the pseudo labels. We set $c = c_t := 1 s \cdot (1 c_0)$ (recall that $\mathbb{P}(L_i = 1) \leq c_0$ under Assumption 3). This is to ensure that the ratio $\frac{c}{1-c}$ correctly accounts for the number of null pseudo targets to training decoys (note, this is not a requirement of FDR/FDX control).
- (v) We record the total number of 'discoveries' produced by SSS over the rK test folds from the previous step and select the classification algorithm that maximizes this value.
- (vi) Using the chosen classification algorithm, we assign new scores \widetilde{W} to the hypotheses. \widetilde{W}_i is defined as the average decision value for the *i*th hypothesis in the test fold that it appears in, taken over the r repetitions executed in Step (iii).
- (vii) We reapply Selective SeqStep (SSS) at α using the pseudo labels and the updated scores, $(\widetilde{L}, \widetilde{W})$ with $c = c_t = 1 s \cdot (1 c_0)$.
- (viii) The positive set is redefined as those pseudo targets that are 'discovered' in Step (vii).

 Steps (ii)-(vi) are then repeated with the new positive set.
- (ix) The final scores \widetilde{W} are then reported.

We refer to the general RESET wrapper in combination with the above semi-supervised approach as *RESET Ensemble*. We refer to *RESET RF/GAM/NN* when the ensemble of machine learning methods in Step (ii) is reduced to a random forest, generalized additive model, and a collection of neural networks as described, respectively.

4.5 Code availability

Our code is available at https://github.com/freejstone/stat_RESET_paper_code with an Apache-2.0 licence. We intend on developing a package for RESET in R.

5 Experiments: competition setting

In the following sections, we explore two applications of competition-based multiple testing. The first is in selecting relevant variables that are conditionally associated with a response. The second is in the detection of peptides from mass spectrometry data.

5.1 Variable selection

We conducted a wide range of simulations in the variable selection problem, where the goal is to identify relevant variables from $\{X_i : i = 1, ..., p\}$ that are conditionally associated to the response y. The variable selection problem uses a competition framework called the knockoff filter (Barber and Candès (2015); Candès et al. (2018)). Briefly, each variable X_i is paired with an artificial knockoff variable, denoted as \tilde{X}_i . Each variable and knockoff is scored according to how well it correlates with the response y, producing Z_i and \tilde{Z}_i , respectively. Then following Section 2, the pairs of scores can be converted into a winning score W_i and a label L_i , and a competition-based multiple testing procedure can be applied (see Section C.3 for details).

The following simulations, detailed in Section C.5, are based on those introduced by Ren and Candès (2023). Each setup, is designed to satisfy Assumption 3, and in each we compare RE-SET Ensemble with Adaptive Knockoffs (AdaKO, with its default GAM filter, see Section C.4 for details), as well as with the generic Knockoff Filter (KO) focusing on FDR control.

- In simulation 1 we consider a linear model with n = 1000 observations with p = 900 variables. We use one dimensional side-information \mathbf{x}_i where lower values correspond to a greater chance of being a relevant feature ($\beta_i \neq 0$). We vary the number of relevant variables $k \in \{50, 150, 300\}$ and generate and analyze 100 datasets for each.
- In simulation 2 we consider a larger linear model with n = 2000 and p = 1800 with two-

dimensional side information. The side information is drawn from a joint normal distribution, with different mean vectors for the relevant and irrelevant variables respectively. We vary the number of relevant variables $k \in \{150, 300, 450\}$ and generate and analyze 20 datasets for each.

- In simulation 3 we consider a high-dimensional logistic model with n = 1000 observations and p = 1600 variables. Relevant and irrelevant variables are determined according to the spatially dependent two-dimensional side information $\mathbf{x}_i = (\mathbf{x}_{i1}, \mathbf{x}_{i2})$ (see Figure C9). We generate and analyze 100 datasets.
- In simulation 4 we consider a linear model with n = 10K observations and p = 10K variables with k = 0.15p relevant variables and three dimensional side information $\mathbf{x_i} = (\mathbf{x}_{i1}, \mathbf{x}_{i2}, \mathbf{x}_{i3})$. Lower values of the \mathbf{x}_{ij} 's correspond to a greater chance of being a relevant feature. We generate and analyze 5 datasets.

5.1.1 Results

In Figure 1, for each simulation we plot the power of each method as a function of the selected FDR thresholds of $\alpha \in \{0.05, 0.1, 0.2, 0.3\}$. The power is calculated as the proportion of relevant variables correctly discovered, averaged over the number of datasets drawn for each simulation. Unsurprisingly, RESET Ensemble uniformly dominates KO, demonstrating that it successfully leverages the side information. At the same time, AdaKO GAM mostly improves on KO, with some exceptions.

In Simulation 1, we find that at higher FDR thresholds, RESET Ensemble is the preferred approach in terms of power. On the other hand, AdaKO GAM is more powerful than RESET at lower FDR thresholds, particularly in the case of k = 50 and $\alpha = 5\%$. This is not too surprising for two reasons. First, RESET trains its classification algorithms on a relatively small positive set of false nulls. Second, RESET incurs a greater cost in terms of power at lower FDR thresholds if the classification algorithm overfits and incorrectly scores a knockoff win higher than it should. Indeed, at an FDR threshold of $\alpha = 5\%$, each knockoff win may cost up to $2/\alpha = 40$ discoveries.

We find in Simulations 2 and 3 that RESET Ensemble is consistently more powerful than AdaKO



Figure 1: Comparing the power of RESET Ensemble, AdaKO GAM and KO. Each panel shows the power of each method at FDR thresholds ranging from 5% to 30%. The first row corresponds to Simulation 1 with three values of $k \in \{50, 150, 300\}$, the second row corresponds to Simulation 2 with three values of $k \in \{150, 300, 450\}$, and the last row corresponds to Simulation 3 and 4. For readability, the points are jittered in the horizontal direction.

GAM; in fact, AdaKO GAM appears to essentially have the same power as KO. Indeed, The result in Simulation 3 is consistent with the findings of Ren and Candès in their analogous simulation. AdaKO GAM does not implement any smooth terms when the number of side information variables is two or more, effectively reducing to a linear model, and is therefore unable to leverage the side information if the true and false null hypotheses are not 'easily' separable. Finally in Simulation 4, we see that RESET Ensemble is generally the most powerful, with essentially the same power

as AdaKO GAM at $\alpha = 5\%$. We hypothesize that the greater number of variables in this example, particularly relevant variables, appears to overcome the relatively poor performance of RESET Ensemble in Simulation 1 at low FDR thresholds.

We compared RESET Ensemble with AdaKO GAM because those are the respective default methods. In Section E.1, we complement this comparison where we summarize the performance of all RESET and AdaKO methods, and also analyze the runtimes of those methods.

5.2 Application to peptide detection

The end-to-end strategy for identifying peptides in an unknown sample can be broken into three steps: data acquisition, search, and competition-based multiple testing. We next provide a brief summary on each of these steps with details given in Section C.6.

During data acquisition, peptides are isolated and selected from a sample where each peptide generates a spectrum using a technique called liquid chromatography mass spectrometry (LC-MS/MS). In the search phase, each spectrum is searched against a database of peptides, called target peptides, for a possible candidate peptide that generated the spectrum. This search phase allows us to provide each target peptide with a score, Z_i , which quantifies evidence against the null hypothesis H_i that 'the target peptide is not in the sample'. Since not all target peptides are in the sample, each spectrum is searched against a database of artificially constructed peptides, called decoy peptides. The decoy peptides are obtained by randomly shuffling or reversing the target peptides. Each decoy peptide is therefore paired with a corresponding target peptide, and acquires a similar score from the search, \tilde{Z}_i .

In the final testing phase, we obtain a winning score, $W_i = Z_i \vee \tilde{Z}_i$ and a label L_i indicating whether the *i*th target peptide $(L_i = 1)$ or its corresponding decoy peptide $(L_i = -1)$ scored higher. We can then apply the SSS+ procedure — with c = 1/2 and α typically set to the 1% FDR threshold — to L and W to obtain a list of target peptides believed to be in the sample. Note that the SSS+ procedure (with c = 1/2) is commonly referred to as target-decoy competition or TDC in the proteomics community.

In the following results, we show that (a) the Adaptive Knockoff methods are often computationally infeasible in this context, and (b) feasibility aside, RESET is more powerful than Adaptive

Table 2: The average runtimes for each method at 1% FDR on the HEK293 dataset.

Method	Time
RESET Ensemble	17.7 minutes
AdaKO GAM	$1.07 \mathrm{days}$
AdaKO EM	34.17 days
AdaKO LR	$3.50 \mathrm{days}$
AdaKO RF	846.33 days

Knockoff's default filter, AdaKO GAM, when controlling the FDR. In Section F.2, we provide a heuristic justification of Assumption 3, which is required for RESET's theoretical guarantees. In terms of FDX control, RESET typically discovers more peptides than the side-information-oblivious FDP-SD (Section E.3). As outlined in Section 4.2, these comparative analyses of RESET Ensemble are new and were not undertaken in Freestone et al. (2025).

5.2.1 Runtime comparison

We argue that the application of Adaptive Knockoffs is often too slow to be used effectively in scenarios such as the peptide detection problem that involve a large amount of data. We demonstrate this using HEK293 (Chick et al. (2015)), a popular dataset used in benchmarking the development of new software (Kong et al. (2017); Yu et al. (2020); Lazear (2023)) that we downloaded from the Proteomics Identification Database (PRIDE) (Martens et al. (2005)). Details regarding the HEK293 dataset and the search phase analysis are given in Section D.1.

We estimated the time it would take for each method of Adaptive Knockoffs to report discoveries at the 1% FDR level (see Section C.14). Table 2 shows the estimated times averaged over 5 different constructions of the decoy database by randomly shuffling the target peptides. All the implementations of AdaKO are not practical for analyzing this data, with the worst being AdaKO RF at an estimated 846.33 days, and the default method, AdaKO GAM, taking an estimate of 1.07 days. In contrast, we were able to run RESET Ensemble in 17.7 minutes on average using 20 cores (Section C.13).

5.2.2 Power comparison

General applicability aside, we resorted to using small datasets to evaluate the power of Adaptive Knockoffs in the peptide detection context. Specifically, we focused on the thirteen smallest datasets from PRIDE-20, a collection of twenty datasets that we recently used (Freestone et al. (2024)). For each of the thirteen spectrum files in PRIDE-20, we performed two types of searches: a narrow and an open search. Briefly, in a narrow search, spectra can only match database peptides that are within a small tolerance of the machine-reported mass of the molecules that generated those spectra. On the other hand, in open searches the same tolerance is several orders of magnitude larger. Details regarding PRIDE-20 and the search settings are given in Section D.2.

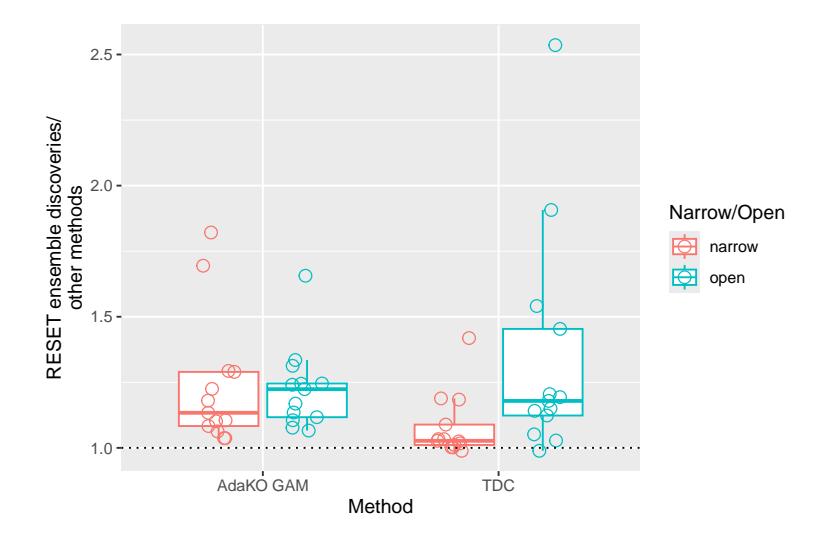


Figure 2: Comparison of RESET Ensemble to AdaKO GAM and TDC. For each of the PRIDE-20 datasets, we computed the average number of discoveries using 10 applications of RESET Ensemble, varying RESET's internal seed. The figure shows a boxplot of those RESET Ensemble averages divided by the number of discoveries using AdaKO GAM (left boxplots) and TDC (right boxplots) applied to thirteen PRIDE-20 datasets and two different search modes (there are total of 13 points in each boxplot).

Figure 2 shows the average number of discoveries reported using RESET Ensemble divided by the number of discoveries reported by AdaKO with its default GAM filter (left boxplots) and TDC (right boxplots), using the two different search settings. We averaged RESET Ensemble over 10 applications by varying the internal seed which randomly splits the decoys into their training and estimating sets. Clearly, RESET Ensemble is overall more powerful than AdaKO GAM and TDC. Interestingly, the relative ratios of the number of discoveries between AdaKO GAM and TDC suggest that AdaKO GAM is at times reporting fewer discoveries than the generic TDC.

In Section E.2, we compare RESET Ensemble with AdaKO RF since we found AdaKO RF to be the most powerful variant of Adaptive Knockoffs in this setting. The results show that RESET Ensemble is comparable to AdaKO RF in terms of power, with the latter still being generally too slow to be practical.

6 Experiments: p-value setting

6.1 Assumption guaranteeing finite-sample FDR control

Recall that RESET and Assumption 3 that guarantees its finite-sample error control are formulated in terms of the labels and winning score (L, W). To apply RESET in the p-value setting, we first convert each p_i into a pair (L_i, W_i) as in Equation (4). Similarly, instead of Assumption 3 we adopt the following assumption formulated by Chao and Fithian (2021) who also showed it implies the former assumption (the next lemma).

Assumption 4. Let N be the indices of the true null hypotheses. Conditioned on the side information \mathbf{x} , and the false null p-values $(p_i)_{i \notin N}$, the true null p-values $(p_i)_{i \in N}$ are independent and have a non-decreasing density.

Lemma 2 (Chao and Fithian). Assumption 4 implies Assumption 3 with $c_0 = \frac{a}{a+b_2-b_1}$, where [0,a) and $(b_1,b_2]$ are the regions corresponding to the positive and negative labels as described in Equation (4).

The above lemma is phrased differently by Chao and Fithian (2021) and is presented as Lemma A.1 in their paper, but it is materially the same. Most of the time, we will consider symmetric cutoff regions [0, 1/2) and (1/2, 1]. For completeness, we provide a proof of this lemma in Section B.2 using our notation.

6.2 Simulated data

In this section, we consider the p-value setting, comparing RESET with the procedures we introduced in Section 3.1 on a set of simulations introduced by Lei and Fithian (2018). Each setup,

detailed through Sections C.7–C.11, is designed to satisfy Assumption 4 and hence Assumption 3, which is required for our theoretical guarantees.

6.2.1 Simulation 5: p-value based testing with geometric side information

In this section, we look at Simulation 1 of Lei and Fithian (2018). For each hypothesis, they obtain a p-value p_i from a one-sided normal test so that $p_i = 1 - \Phi(z_i)$ where $z_i \sim \mathcal{N}(\mu, 1)$ with $\mu = 2$ for a false null hypothesis and $\mu = 0$ for a true null hypothesis. A total of m = 2500 hypotheses are used. Each hypothesis' side information is defined as a unique pair of values $\mathbf{x}_i = (\mathbf{x}_{i1}, \mathbf{x}_{i2})$ from 50×50 equally spaced values in the square $[-100, 100] \times [-100, 100]$. The false null hypotheses correspond to certain regions in the square. They considered three scenarios: (a) when the false nulls form a circle in the middle of the square, (b) when the false nulls form a circle in the top right of the square and (c) when the false nulls form an ellipse (Figure C12). We generated and analyzed 100 independent datasets, where in each we randomly draw the 2500 p-values as described.

Figure 3 shows the results of RESET compared with several p-value based methods that we reviewed in Section 3.1. We find that in the first two simulations, (a) and (b), RESET Ensemble is roughly equal to the best method in terms of power at the 5%, 10% and 20% FDR levels, along with AdaPT/AdaPT_g GAM. However, in (c), clearly AdaPT/AdaPT_g GAM are more powerful than the RESET methods, with RESET Ensemble coming arguably as third in the power ranking at the 5%, 10%, and 20% FDR levels. At 1% FDR, all RESET methods have negligible power, although this is consistent with many of the other methods. Interestingly, many of the finite-FDR controlling procedures such as the various RESET and AdaPT methods generally have better power than the asymptotic approaches, ZAP and AdaFDR, suggesting perhaps a misspecification of the fitted model used by these approaches. Figure 3 also shows the estimated FDR of each method. We find that in (a), AdaFDR's estimated FDR at 20% (21.2% estimated FDR with 50% power) slightly exceeds the FDR threshold. This is possibly explained by the fact that AdaFDR only guarantees asymptotic FDX control. Consistently, Chao and Fithian (2021) reported inflated estimated FDRs at high thresholds in simulation studies for AdaFDR.

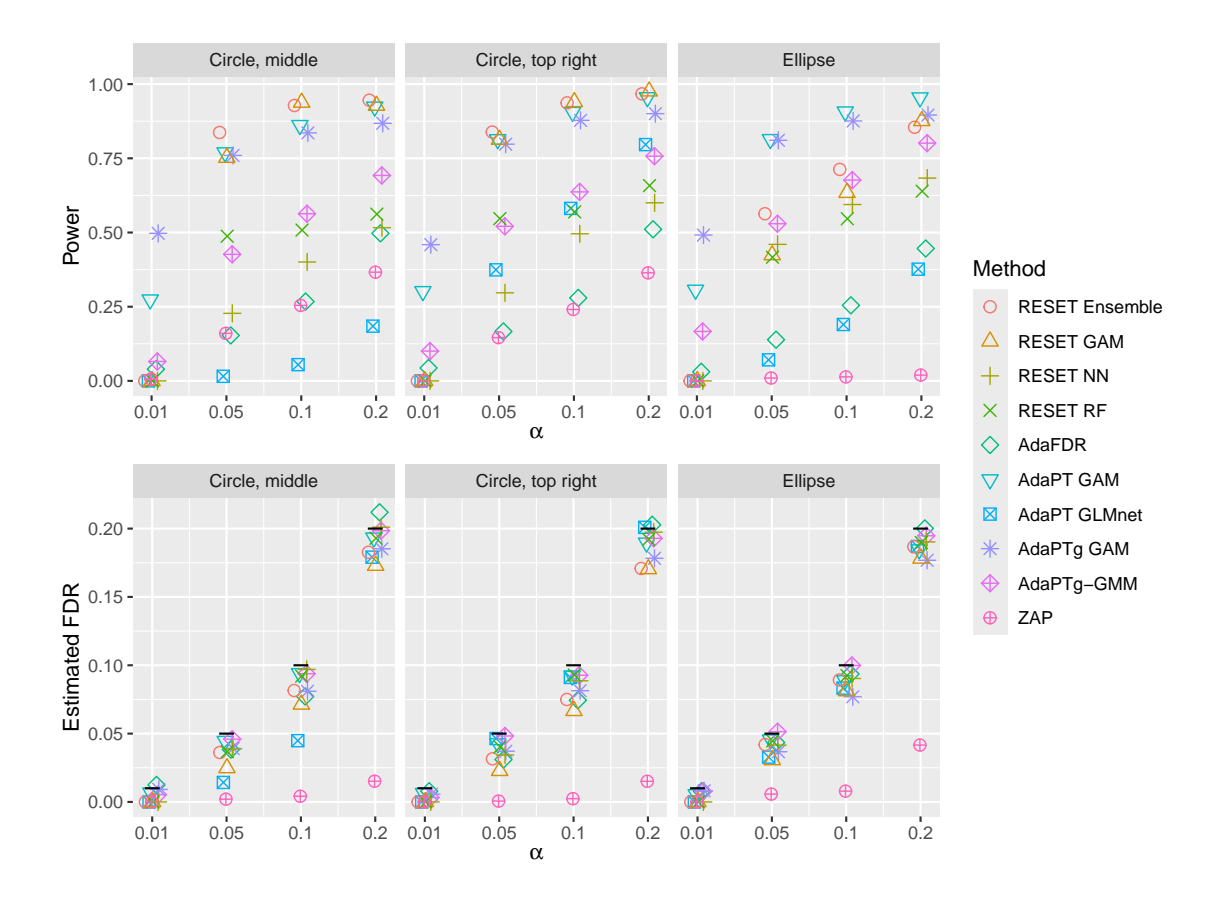


Figure 3: RESET vs. other methods using p-values with two-dimensional side information. The power (1st row) and the estimated FDR (2nd row) are plotted against FDR thresholds ranging from 1% to 20%. Each color and shape combination corresponds to a unique method. The three columns correspond to the hypotheses' relationship to the side information according to Figure C12. The black horizontal segments in the second row of panels mark the corresponding FDR thresholds on the y-axis. For readability, each point is jittered in the horizontal direction.

6.2.2 Simulation 6: p-value based testing with 100-dimensional side information

We next adopted Simulation 2 of Lei and Fithian (2018). The side information for m = 2000 hypotheses consists of 100 *i.i.d.* draws from U[0,1] in which only the first 2 of the 100 draws are used in distinguishing between the true and false null hypotheses. Details are given in Section C.12. We conducted 100 independent runs, where in each run we randomly draw the m = 2000 p-values.

There were a couple of tools we had to omit from the analysis of this data. Surprisingly, we found that AdaFDR was too slow in this simulation. Similarly, we were not able to apply AdaPT GAM or AdaPT_g GAM as we did in the previous simulation, since it would have required using a smoothing spline on all 100 side-information variables, which is impractical. Hence, we only applied the GLMnet variants of AdaPT.

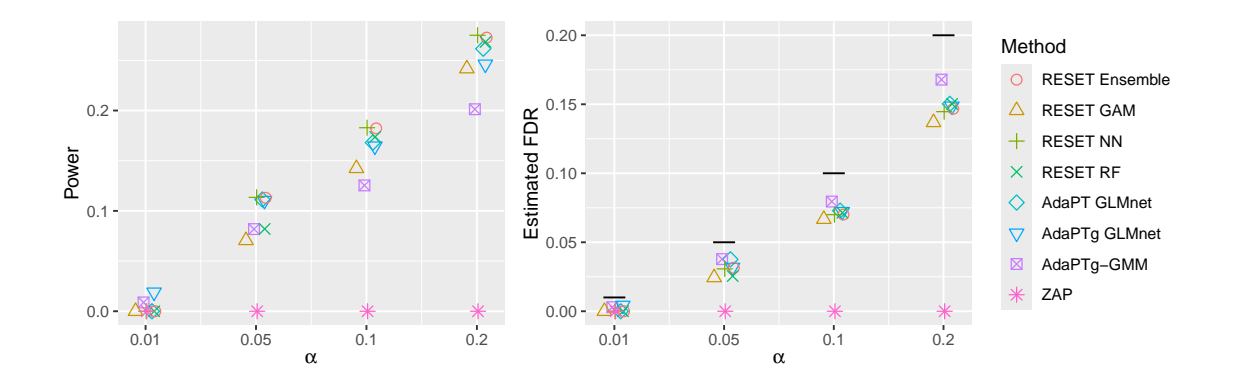


Figure 4: RESET vs. other methods using p-values with 100-dimensional side information. The power (left panel) and the estimated FDR (right panel) are plotted as a function of the FDR thresholds: 1%, 5%, 10% and 20%. Each color and shape combination corresponds to a unique method. The black horizontal segments in the right panel mark the corresponding FDR thresholds on the y-axis. For readability, each point is jittered in the horizontal direction.

Examining Figure 4, which graphically summarizes this analysis, it appears that RESET Ensemble, RESET NN, and AdaPT GLMnet deliver the most discoveries at the 5%, 10%, and 20% FDR levels. At 1% FDR, only AdaPTg GLMnet appears to have non-negligible power, albeit a fairly low number of discoveries. Finally, we point out that in this simulation, the model specification of AdaPT/AdaPTg perfectly matches the underlying data generating model: the fitted mixture model used by AdaPT/AdaPTg coincides with Equation (7) of Section C.12. Given this, we find it reassuring that RESET Ensemble is still comparable at 5% and higher thresholds.

Notably, the performance of AdaPT in these last two simulation setups is highly dependent on the choice of implementation. In Simulation 5, AdaPT GAM significantly outperforms AdaPT GLMnet while in Simulation 6, AdaPT GLMnet is superior and AdaPT GAM is not even practical. In contrast, RESET Ensemble selects from a collection of flexible machine learning models to adapt itself to the problem at hand.

6.3 Robustness to dependent data

In reality, real datasets often exhibit varying degrees of dependency, therefore failing to satisfy Assumptions 3 and 4. RESET Ensemble is equipped with a heuristic to account for such data (Section C.2.4). The following simulations adapted from Zhang et al. (2019) empirically demonstrate that RESET Ensemble exhibits some robustness to both weak and strong forms of local dependency.

6.3.1 Simulation 7: Weak dependent p-values

This simulation is based on Data 4 of Zhang et al. (2019). We generated m=20K hypotheses with i.i.d side information drawn from $\mathbf{x}_i \sim U[0,1]$. Each hypothesis was declared a false null with probability $\pi_i := \pi(\mathbf{x}_i)$ which is dependent on the drawn side-information. The function π is a convex combination of (truncated) normal densities and an exponential function (Section C.12.2). For every 10 consecutive hypotheses, starting with $i=1,\ldots,10$, we drew z_i jointly from a $\mathcal{N}(0,\Sigma)$ where Σ is a covariance matrix with upper triangular matrix given by $\Sigma_{jj}=1$, $\Sigma_{jk}=0.25$ for $1 \leq j < k \leq 5$, $\Sigma_{jk}=-0.25$ for $1 \leq j \leq 5 < k \leq 10$ and $\Sigma_{jk}=0$ for all other entries in the upper triangle. Hypotheses which are false nulls had their z-scores shifted by 2. A one-sided p-value $p_i=1-\Phi(z_i)$ is then obtained. Notably, the covariance matrix Σ induces a local weak dependency among the p-values, effecting both true and false null hypotheses.

6.3.2 Simulation 8: Strong dependent p-values

This simulation is based on Data 5 of Zhang et al. (2019). We used m=20K hypotheses with side information \mathbf{x}_i and false null probability π_i defined as in Simulation 7. For every 5 consecutive hypotheses, starting with $i=1,\ldots,5,\,z_i=z$ where $z\sim\mathcal{N}(0,1)$, creating 5 identical z-scores. False null hypotheses are shifted by 2 and one-sided p-values $p_i=1-\Phi(z_i)$ were obtained. In this case, the data exhibits a local strong dependency effecting both true and false null p-values.

6.3.3 Results

Figure 5 shows the estimated FDR calculated from 100 runs of the above simulations. In the weakly dependent case (A), the majority of the methods seem to empirically control the FDR, with the exception of AdaFDR and RESET GAM which appears to marginally exceed the 5% threshold. In the strongly dependent data (B), we see several more methods exceeding their respective thresholds, albeit relatively mildly. RESET Ensemble seems to be robust and appears to approximately control the FDR in these experiments.

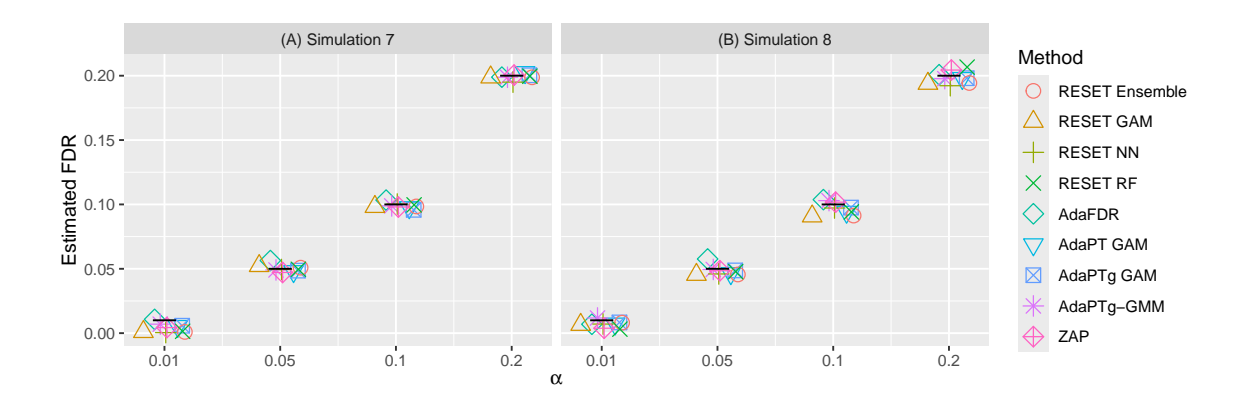


Figure 5: Estimated FDR using RESET vs. other methods on dependent p-values. The estimated FDR is plotted as a function of the FDR thresholds: 1%, 5%, 10% and 20% for weak (A) and strong dependence (B). Each color and shape combination corresponds to a unique method. The black horizontal segments mark the corresponding FDR thresholds on the y-axis. For readability, each point is jittered in the horizontal direction.

6.4 Real data experiments with p-values

We next evaluate RESET and related methods on a collection of publicly available datasets with p-values. These were investigated by Zhang et al. (2019), when introducing AdaFDR, and by Lei and Fithian (2018) when introducing AdaPT. A description of each dataset can be found in Section D.3.

As we saw above, RESET Ensemble and the other tools we analyze here exhibit some robustness to deviations from the independence assumption that is built into Assumptions 3 and 4. However, despite this fact, we sought to remove the two Adipose datasets from this analysis because RESET's heuristics, described in Section C.2.4, flagged these datasets for high dependency (cf. Section F.3).

For each dataset (excluding the two Adipose datasets) and each FDR threshold in {1%, 5%, 10%, 20%}, we computed the maximum number of discoveries across all methods and determined the power of each method relative to this maximum (Figure 6). RESET Ensemble (94.4%), RESET NN (93.6%) and AdaPT_g-GMM (91.5%) have the highest medians, with RESET Ensemble also arguably having the tightest boxplot. Figure E6 shows the number of discoveries for each method on each of the 40 combinations of dataset and FDR threshold.

There are a couple of implementation comments we highlight here (see Sections C.7-C.11 for details). First, we used the same default options of RESET Ensemble for all datasets, except for the two fMRI datasets which exhibit a spike of p-values close to 1. To address this, we followed Chao and Fithian (2021)'s suggestion of defining asymmetric target and decoy regions of [0, 0.3) and

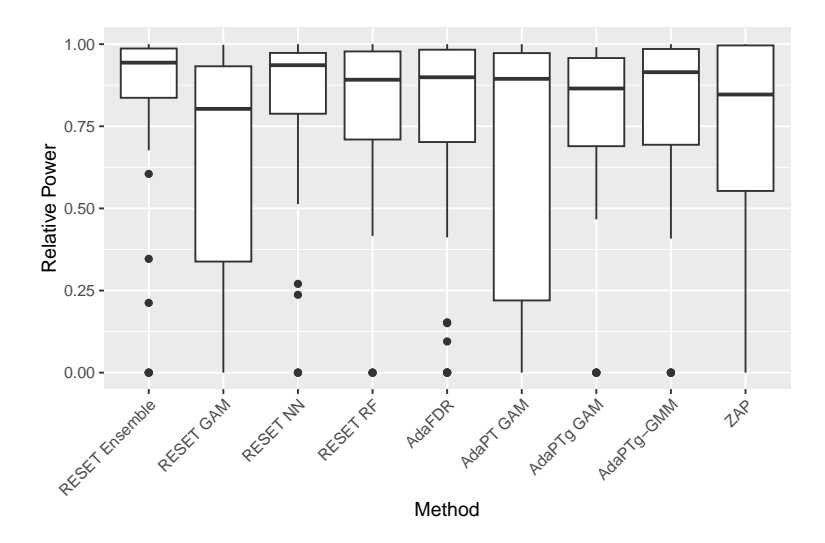


Figure 6: Power comparison. Each boxplot is made of 40 data points showing the relative power of a method on all combinations of dataset and FDR threshold. There are ten dataset as described in Section D.3 (excluding the two Adipose datasets) and four FDR thresholds: 1%, 5%, 10% and 20%. RESET Ensemble's power and its variants were averaged over 10 applications.

(0.3, 0.9] respectively. Second, we applied AdaPT_g-GMM and ZAP using the p-value information rather than the test statistic information. To do so, AdaPT_g-GMM allows the user to directly input p-values instead of z-statistics. For ZAP, we converted the p-value information into z-values by defining $z_i = \pm \Phi^{-1}(p_i/2)$ for each p-value, p_i , where the signs are chosen *i.i.d.* uniformly. In other words, we input plausible z-values that correspond to the same p-value information used by the other tools. As we mentioned in Section 3, our implementation of RESET focuses on the use of p-values, and we leave the extension to test statistic information as part of future work.

To evaluate the runtime of each method, we used the two fMRI datasets, which use the largest number of side information variables and has a large number of hypotheses. Figure 7(A-B) shows the runtimes for each considered method, where the fastest are the collection of RESET methods, ZAP and AdaFDR. RESET NN, RESET GAM and RESET RF are slightly faster than our ensemble approach which considers all of them.

6.5 FDX control with p-values

In this final section, we demonstrate RESET's FDX control in the p-value setting. To the best of our knowledge, there are no existing p-value-based testing procedures that offer finite sample FDX control while utilizing side information. Therefore, we compare RESET Ensemble against FDP-

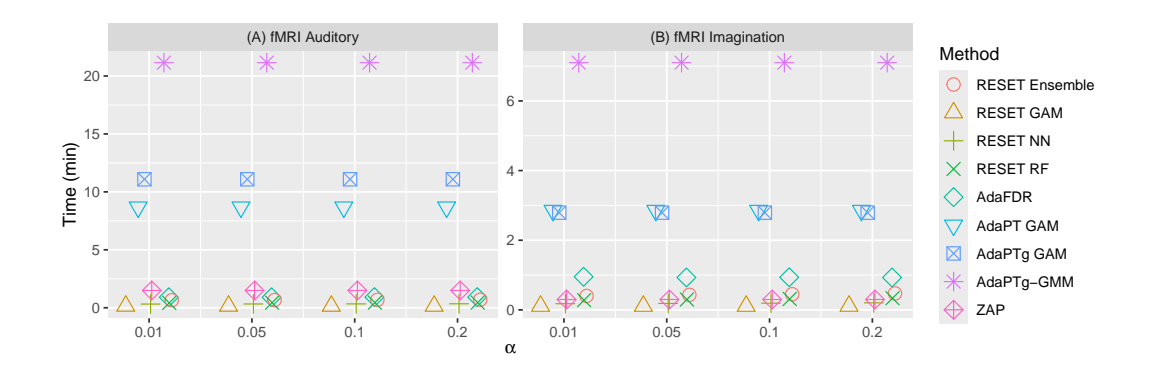


Figure 7: Runtime comparison. In (A) and (B), we compare the runtime of each method on the fMRI datasets. We averaged the times of each RESET method over 10 applications.

SD (Algorithm A2) and GR-SD (Algorithm A3). The labels and scores (L, W) used in RESET Ensemble and FDP-SD are defined using the asymmetric target and decoy regions—[0, 0.3) and (0.3, 0.9], respectively—for all datasets. The rationale stems from our analysis in Section F.4, which points out that when the ratio of estimating decoys to true null targets is small, RESET might incur a loss of power when controlling the FDX. To rectify this, we define a decoy region that is twice as large as the corresponding target region.

Figure 8 displays the number of discoveries obtained by each method on the collection of real datasets we considered in the previous section. The numbers are averaged over 10 runs while varying the FDR thresholds (1%, 5%, 10%, 20%) and the confidence levels (50%, 80%, 90%). With a few exceptions RESET Ensemble is generally much more powerful than the alternative approaches that make no use of the side information.

7 Discussion

RESET provides a general framework for FDR and FDX control through a flexible wrapper for any semi-supervised learning algorithm. Alongside, we introduced an implementation of RESET, called RESET Ensemble, that is power-wise competitive with recently developed methods for competition as well as p-value based multiple testing problems with side information, is fast compared to most tools, and is flexible allowing finite sample FDR and FDX control.

In terms of power, we highlight the fact that competing tools, such as the variants of AdaPT or Adaptive Knockoffs, require an initial selection of one of those variants. Making a selection

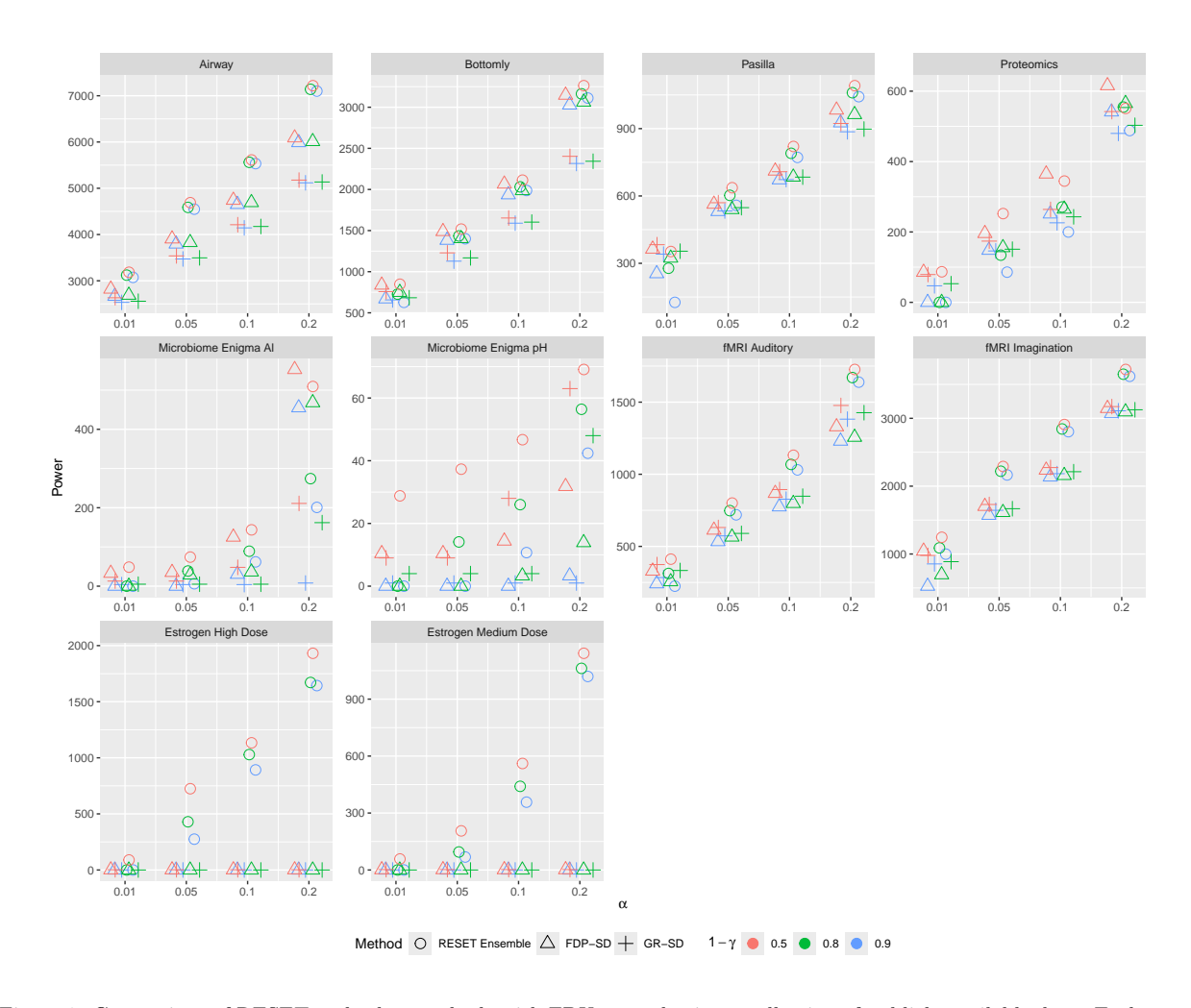


Figure 8: Comparison of RESET and other methods with FDX control using a collection of publicly available data. Each panel shows the number of discoveries obtained by RESET Ensemble, FDP-SD and GR-SD at a range of FDR thresholds (1%, 5%, 10%, 20%) with varying confidence $1-\gamma$ (0.5, 0.8, 0.9). RESET Ensemble and FDP-SD were averaged over 10 applications.

after observing the discovery lists of each tool will generally compromise its FDR control. Thus, we compared RESET Ensemble to the default competing method if one was available, which is the case with Adaptive Knockoff's GAM filter, or *separately* to each variant, which is the case for AdaPT. Based on our comparisons, we conclude that RESET Ensemble is able to achieve comparable or slightly greater power than many of these tools while freeing the user from having to choose the 'right' method to begin with.

We found that each of our RESET methods was consistently faster than any of the competing methods for finite FDR control with side-information we considered here. More generally, the only case in which RESET was surpassed in terms of speed was ZAP-asymp, which demonstrated marginally faster runtimes than RESET Ensemble in one of the fMRI datasets (Figure 7B). How-

ever, ZAP-asymp's fast runtimes come at the cost of asymptotic FDR control. The most striking difference in runtimes was in the peptide detection context using mass spectrometry data, in which all variants of Adaptive Knockoffs were generally too slow to be practical. RESET's impressive speed compared to Adaptive Knockoffs and the AdaPT variants is due to the fact that these methods work by iterating between training a classification algorithm, and deciding which hypothesis to remove from the candidate set \hat{S}_t as explained in Section 2.1. In contrast, RESET Ensemble can be heavily parallelized, and only performs two iterations.

Finally, we point out that RESET's compatibility with FDR as well as FDX control is unique. In the competition setting, we note that it would be challenging to combine Adaptive Knockoffs with FDP-SD because FDP-SD is a stepdown procedure while Adaptive Knockoffs is essentially a step-up procedure. Katsevich and Ramdas (2020) provide a general method for adaptive ordering using their method for simultaneous FDP bounds. However, (a) they do not provide an exact implementation of this, only a theoretical discussion, and (b) their approach is conservative since it controls the FDX at every cutoff (which allows the analyst to explore the nested discovery lists without breaking FDX control). To the best of our knowledge, in the competition framework with side information, RESET is the only method of reordering that may be flexibly used with FDP-SD without the additional cost of (b). Similarly, we know of no method that allows finite sample FDX control in the p-value setting with side information.

Notably, RESET's discovery list is variable since it randomly splits the decoys into two sets: one set for training and the other for estimating the false discoveries. While this is problematic to an extent, keep in mind that the data distribution is random, and the added variance from RESET may be marginal at times (cf. Section F.5).

Lastly, we point out a few avenues for further research. While RESET is a flexible method for the competition and p-value based testing, we wish to further extend it to the test-statistic setting. There is more than one way of generalizing RESET to accommodate a test statistic z_i for each hypothesis H_i . Moreover, there are several 'types' of interactions between the side information \mathbf{x}_i and the test statistic z_i which are not preserved when switching to p-values, as outlined by Leung and Sun (2022). Thus it is not clear that RESET Ensemble will be equally applicable in this setting without substantial modifications. Second, RESET relies on a handful of prespecified quantities: the probability s of assigning decoys to the estimation set, and the definitions of the target and decoy regions as [0, a) and $(b_1, b_2]$, respectively. Moreover, in Step (1) we employ a mirroring function that converts larger p-values in the decoy region into smaller values in the target region. Given that the true null p-values are possibly non-uniform, we could consider other masking functions as suggested by Chao and Fithian (2021). The selection of these parameters and the masking function would ideally be data-driven which we leave as part of future work. Finally, we may consider alternatives to our semi-supervised learning engine, RESET Ensemble. One direction is to pair RESET's data-splitting scheme with AdaPT's iterative fitting procedure, which could further increase power (at the expense of additional computation time). Another is to broaden RESET Ensemble's library of classifiers to include the two-group models that are used by many of the competing methods.

References

- Barber, R. F. and Candès, E. J. (2015) Controlling the false discovery rate via knockoffs. *The Annals of Statistics*, **43**, 2055–2085.
- Bates, S., Candès, E., Lei, L., Romano, Y. and Sesia, M. (2023) Testing for outliers with conformal p-values. *The Annals of Statistics*, **51**, 149–178.
- Benjamini, Y. and Hochberg, Y. (1995) Controlling the false discovery rate: a practical and powerful approach to multiple testing. *Journal of the Royal Statistical Society Series B*, **57**, 289–300.
- Benjamini, Y., Krieger, A. M. and Yekutieli, D. (2006) Adaptive linear step-up procedures that control the false discovery rate. *Biometrika*, **93**, 491–507.
- Blanchard, G. and Roquain, E. (2008) Two simple sufficient conditions for fdr control. *Electronic Journal of Statistics*, 2.
- Bottomly, D., Walter, N. A., Hunter, J. E., Darakjian, P., Kawane, S., Buck, K. J., Searles, R. P., Mooney, M., McWeeney, S. K. and Hitzemann, R. (2011) Evaluating gene expression in c57bl/6j and dba/2j mouse striatum using rna-seq and microarrays. *PloS one*, **6**, e17820.
- Brodmann, K. (1909) Vergleichende Lokalisationslehre der Grosshirnrinde in ihren Prinzipien dargestellt auf Grund des Zellenbaues. Barth.
- Brooks, A. N., Yang, L., Duff, M. O., Hansen, K. D., Park, J. W., Dudoit, S., Brenner, S. E. and Graveley, B. R. (2011) Conservation of an rna regulatory map between drosophila and mammals. *Genome research*, **21**, 193–202.
- Candès, E. J., Fan, Y., Janson, L. and Lv, J. (2018) Panning for gold: Model-X knockoffs for high-dimensional controlled variable selection. *Journal of the Royal Statistical Society: Series B* (Statistical Methodology), 80, 551–577.
- Chao, P. and Fithian, W. (2021) Adapt-gmm: Powerful and robust covariate-assisted multiple testing. arXiv preprint arXiv:2106.15812.

- Chick, J. M., Kolippakkam, D., Nusinow, D. P., Zhai, B., Rad, R., Huttlin, E. L. and Gygi, S. P. (2015) A mass-tolerant database search identifies a large proportion of unassigned spectra in shotgun proteomics as modified peptides. *Nature Biotechnology*, 33, 743–749.
- Consortium, G. (2020) The gtex consortium atlas of genetic regulatory effects across human tissues. Science, 369, 1318–1330.
- Consortium, G., Ardlie, K. G., Deluca, D. S., Segrè, A. V., Sullivan, T. J., Young, T. R., Gelfand, E. T., Trowbridge, C. A., Maller, J. B., Tukiainen, T. et al. (2015) The genotype-tissue expression (gtex) pilot analysis: multitissue gene regulation in humans. *Science*, **348**, 648–660.
- Davis, S. and Meltzer, P. S. (2007) Geoquery: a bridge between the gene expression omnibus (geo) and bioconductor. *Bioinformatics*, **23**, 1846–1847.
- Dempster, A. P., Laird, N. M. and Rubin, D. B. (1977) Maximum likelihood from incomplete data via the EM algorithm. *Journal of the Royal Statistical Society. Series B (Methodological)*, **39**, 1–22.
- Dephoure, N. and Gygi, S. P. (2012) Hyperplexing: a method for higher-order multiplexed quantitative proteomics provides a map of the dynamic response to rapamycin in yeast. *Science signaling*, **5**, rs2–rs2.
- Diament, B. and Noble, W. S. (2011) Faster SEQUEST searching for peptide identification from tandem mass spectra. *Journal of Proteome Research*, **10**, 3871–3879.
- Ebadi, A., Luo, D., Freestone, J., Noble, W. S. and Keich, U. (2023) Bounding the FDP in competition-based control of the FDR. arXiv preprint arXiv:2302.11837.
- Elias, J. E. and Gygi, S. P. (2007) Target-decoy search strategy for increased confidence in large-scale protein identifications by mass spectrometry. *Nature Methods*, **4**, 207–214.
- Emery, K., Hasam, S., Noble, W. S. and Keich, U. (2020) Multiple competition-based fdr control and its application to peptide detection. In *International Conference on Research in Computational Molecular Biology*, 54–71. Springer.

- Freestone, J., Käll, L., Noble, W. S. and Keich, U. (2025) How to train a postprocessor for tandem mass spectrometry proteomics database search while maintaining control of the false discovery rate. *Journal of Proteome Research*, **24**, 2266–2279.
- Freestone, J., Noble, W. S. and Keich, U. (2024) Analysis of tandem mass spectrometry data with conga: Combining open and narrow searches with group-wise analysis. *Journal of Proteome Research*, 23, 1894–1906.
- Genovese, C. R., Roeder, K. and Wasserman, L. (2006) False discovery control with p-value weighting. *Biometrika*, **93**, 509–524.
- Goeman, J. J., Hemerik, J. and Solari, A. (2021) Only closed testing procedures are admissible for controlling false discovery proportions. *The Annals of Statistics*, **49**, 1218 1238. URL: https://doi.org/10.1214/20-AOS1999.
- Granholm, V., Noble, W. S. and Käll, L. (2011) On using samples of known protein content to assess the statistical calibration of scores assigned to peptide-spectrum matches in shotgun proteomics.

 Journal of Proteome Research, 10, 2671–2678.
- G'Sell, M. G., Wager, S., Chouldechova, A. and Tibshirani, R. (2016) Sequential selection procedures and false discovery rate control. *Journal of the Royal Statistical Society Series B: Statistical Methodology*, **78**, 423–444.
- Guo, W. and Romano, J. (2007) A generalized sidak-holm procedure and control of generalized error rates under independence. Statistical applications in genetics and molecular biology, 6.
- Habiger, J. D. (2017) Adaptive false discovery rate control for heterogeneous data. *Statistica Sinica*, 1731–1756.
- He, K., Fu, Y., Zeng, W.-F., Luo, L., Chi, H., Liu, C., Qing, L.-Y., Sun, R.-X. and He, S.-M. (2015)

 A theoretical foundation of the target-decoy search strategy for false discovery rate control in proteomics. arXiv. Https://arxiv.org/abs/1501.00537.
- Himes, B. E., Jiang, X., Wagner, P., Hu, R., Wang, Q., Klanderman, B., Whitaker, R. M., Duan, Q., Lasky-Su, J., Nikolos, C. et al. (2014) Rna-seq transcriptome profiling identifies crispld2 as a

- glucocorticoid responsive gene that modulates cytokine function in airway smooth muscle cells. *PloS one*, **9**, e99625.
- Hu, J. X., Zhao, H. and Zhou, H. H. (2010) False discovery rate control with groups. *Journal of the American Statistical Association*, **105**, 1215–1227.
- Huber, W. and Reyes, A. () pasilla: Data package with per-exon and per-gene read counts of rna-seq samples of pasilla knock-down by brooks et al., genome research 2011, r package 1.34.0.
- Ignatiadis, N. and Huber, W. (2021) Covariate powered cross-weighted multiple testing. *Journal* of the Royal Statistical Society Series B: Statistical Methodology, 83, 720–751.
- Ignatiadis, N., Klaus, B., Zaugg, J. B. and Huber, W. (2016) Data-driven hypothesis weighting increases detection power in genome-scale multiple testing. *Nature Methods*, **13**, 577–580.
- Käll, L., Canterbury, J. D., Weston, J., Noble, W. S. and MacCoss, M. J. (2007) Semi-supervised learning for peptide identification from shotgun proteomics datasets. *Nature Methods*, 4, 923–925.
- Katsevich, E. and Ramdas, A. (2020) Simultaneous high-probability bounds on the false discovery proportion in structured, regression and online settings. *The Annals of Statistics*, **48**, 3465 3487. URL: https://doi.org/10.1214/19-AOS1938.
- Kertesz-Farkas, A., Nii Adoquaye Acquaye, F. L., Bhimani, K., Eng, J. K., Fondrie, W. E., Grant, C., Hoopmann, M. R., Lin, A., Lu, Y. Y., Moritz, R. L., MacCoss, M. J. and Noble, W. S. (2023) The Crux Toolkit for Analysis of Bottom-Up Tandem Mass Spectrometry Proteomics Data. Journal of Proteome Research, 22, 561–569.
- Kong, A. T., Leprevost, F. V., Avtonomov, D. M., Mellacheruvu, D. and Nesvizhskii, A. I. (2017) MSFragger: ultrafast and comprehensive peptide identification in mass spectrometry-based proteomics. *Nature Methods*, 14, 513–520.
- Korthauer, K., Kimes, P. K., Duvallet, C., Reyes, A., Subramanian, A., Teng, M., Shukla, C., Alm, E. J. and Hicks, S. C. (2019) A practical guide to methods controlling false discoveries in computational biology. *Genome biology*, 20, 1–21.

- Lazear, M. R. (2023) Sage: An open-source tool for fast proteomics searching and quantification at scale. *Journal of Proteome Research*, **22**, 3652–3659.
- Lei, L. and Fithian, W. (2016) Power of ordered hypothesis testing. In *International Conference* on Machine Learning, 2924–2932.
- (2018) Adapt: an interactive procedure for multiple testing with side information. *Journal of the Royal Statistical Society: Series B (Statistical Methodology)*, **80**, 649–679.
- Leung, D. and Sun, W. (2022) Zap: z-value adaptive procedures for false discovery rate control with side information. *Journal of the Royal Statistical Society Series B: Statistical Methodology*, 84, 1886–1946.
- Li, A. and Barber, R. F. (2017) Accumulation tests for fdr control in ordered hypothesis testing.

 Journal of the American Statistical Association, 112, 837–849.
- (2019) Multiple testing with the structure-adaptive benjamini-hochberg algorithm. *Journal of the Royal Statistical Society Series B: Statistical Methodology*, **81**, 45–74.
- Li, J., Maathuis, M. H. and Goeman, J. J. (2022) Simultaneous false discovery proportion bounds via knockoffs and closed testing. arXiv preprint arXiv:2212.12822.
- Lin, A., Short, T., Noble, W. S. and Keich, U. (2022) Improving peptide-level mass spectrometry analysis via double competition. *Journal of Proteome Research*, **21**, 2412–2420.
- Luo, D., Ebadi, A., Emery, K., He, Y., Noble, W. S. and Keich, U. (2023) Competition-based control of the false discovery proportion. *Biometrics*, **79**, 3472–3484.
- Marandon, A., Lei, L., Mary, D. and Roquain, E. (2024) Adaptive novelty detection with false discovery rate guarantee. *The Annals of Statistics*, **52**, 157–183.
- Martens, L., Hermjakob, H., Jones, P., Adamsk, M., Taylor, C., States, D., Gevaert, K., Vandeker-ckhove, J. and Apweiler, R. (2005) PRIDE: The proteomics identifications database. *Proteomics*, 5, 3537–3545.

- Nesvizhskii, A. I. (2010) A survey of computational methods and error rate estimation procedures for peptide and protein identification in shotgun proteomics. *Journal of Proteomics*, **73**, 2092 2123.
- Park, C. Y., Klammer, A. A., Käll, L., MacCoss, M. P. and Noble, W. S. (2008) Rapid and accurate peptide identification from tandem mass spectra. *Journal of Proteome Research*, 7, 3022–3027.
- Ramdas, A. K., Barber, R. F., Wainwright, M. J. and Jordan, M. I. (2019) A unified treatment of multiple testing with prior knowledge using the p-filter. *The Annals of Statistics*, **47**, 2790–2821.
- Ren, Z. and Candès, E. (2023) Knockoffs with side information. *The Annals of Applied Statistics*, 17, 1152–1174.
- Roquain, E. and Van De Wiel, M. A. (2009) Optimal weighting for false discovery rate control.

 Electronic Journal of Statistics, 3, 678–711.
- Sesia, M., Sabatti, C. and Candès, E. J. (2019) Gene hunting with hidden markov model knockoffs. *Biometrika*, **106**, 1–18.
- Smith, M. B., Rocha, A. M., Smillie, C. S., Olesen, S. W., Paradis, C., Wu, L., Campbell, J. H., Fortney, J. L., Mehlhorn, T. L., Lowe, K. A. et al. (2015) Natural bacterial communities serve as quantitative geochemical biosensors. MBio, 6, 10–1128.
- Storey, J. D., Taylor, J. E. and Siegmund, D. (2004) Strong control, conservative point estimation, and simultaneous conservative consistency of false discovery rates: A unified approach. *Journal of the Royal Statistical Society, Series B*, **66**, 187–205.
- Sulimov, P. and Kertész-Farkas, A. (2020) Tailor: A nonparametric and rapid score calibration method for database search-based peptide identification in shotgun proteomics. *Journal of Proteome Research*, **19**, 1481–1490.
- Tabelow, K. and Polzehl, J. (2011) Statistical parametric maps for functional mri experiments in r: The package fmri. *Journal of Statistical Software*, **44**, 1–21.
- Tibshirani, R. J. (1996) Regression shrinkage and selection via the lasso. *Journal of the Royal Statistical Society B*, **58**, 267–288.

- Yu, F., Teo, G. C., Kong, A. T., Haynes, S. E., Avtonomov, D. M., Geiszler, D. J. and Nesvizhskii, A. I. (2020) Identification of modified peptides using localization-aware open search. *Nature Communications*, 11, 4065.
- Zhang, M. J., Xia, F. and Zou, J. (2019) Fast and covariate-adaptive method amplifies detection power in large-scale multiple hypothesis testing. *Nature communications*, **10**, 3433.

Supplement

A Algorithms

Algorithm A1 Selective SeqStep / SeqStep+ (adopted from Selective Sequential Step+ of Barber and Candès (2015))

```
Input: • (L_i, W_i)_{i=1}^m the list of paired winning labels and scores;

• c \in (0, 1) - the probability of a null target/feature win;

• \alpha \in (0, 1) - the FDR threshold;

Output: A discovery list R_{\alpha}

1: sort the paired (L_i, W_i) in decreasing order of W_i \triangleright ties are randomly broken

2: A_t \leftarrow \#\{i \le t : L_i = -1\} \triangleright number of decoy/knockoffs wins in top t scores

3: R_t \leftarrow \#\{i \le t : L_i = 1\} \triangleright number of target/original feature wins in top t scores

4: if SeqStep then

5: \tau \leftarrow \max\{t : \frac{A_t}{R_t \lor 1} \cdot \frac{c}{1-c} \le \alpha\}

6: else if SeqStep+ then

7: \tau \leftarrow \max\{t : \frac{A_t + 1}{R_t \lor 1} \cdot \frac{c}{1-c} \le \alpha\}

8: end if

9: return R_{\alpha} \leftarrow \{i : \text{the (pre-sorted)} \ W_i \text{ is in the top } \tau \text{ ranks and } L_i = 1\}
```

Algorithm A2 FDP-SD (adopted from Luo et al. (2023))

```
Input: • (L_i, W_i)_{i=1}^m the list of paired winning labels and scores;
              • c \in (0,1) - the probability of a null target/feature win;
               • \alpha \in (0,1) - the FDP threshold;
               • \gamma \in (0,1) - for a 1-\gamma confidence level;
Output: A discovery list R_{\alpha,\gamma}
 1: sort the paired (L_i, W_i) in decreasing order of W_i

    b ties are randomly broken

 2: \lambda \leftarrow c
 3: R \leftarrow (1 - \lambda)/(c + 1 - \lambda)
 4: i_0 \leftarrow \max\{1, \lceil(\lceil \log_{1-R}(\gamma)\rceil)/\alpha\rceil\}
 5: for i = i_0, ..., m do
           A_i \leftarrow \#\{j \le i : L_j = -1\}
                                                                                            \triangleright number of decoy wins in top i scores
                                                                                                        \triangleright F_{B(n,p)} denotes the CDF of a
           \delta_i \leftarrow \max\{d \in \{0, 1, \dots, i\} : F_{B(|(i-d)\alpha+1+d, R|)}(d) \le \gamma\}
      Binomial(n, p) RV
 8: end for
 9: i \leftarrow i_0 and \delta_{i_0-1} \leftarrow -1 and \bar{\delta}_{i_0-1} \leftarrow 0
10: while i \leq m do
           k_0 \leftarrow |(i - \delta_i) \cdot \alpha| + 1
11:
           k_1 \leftarrow |(i - \delta_i + 1) \cdot \alpha| + 1
12:
           p_0 \leftarrow F_{B(k_0 + \delta_i, R)}(\delta_i)
13:
           p_1 \leftarrow F_{B(k_1+\delta_i+1,R)}(\delta_i+1)
14:
           w_i \leftarrow (p_1 - \gamma)/(p_1 - p_0)
15:
           if \bar{\delta}_{i-1} = \delta_i + 1 then
16:
                \bar{\delta}_i \leftarrow \bar{\delta}_{i-1}
17:
           else
18:
                if \delta_i > \delta_{i-1} then
19:
                      w' \leftarrow w_i
20:
21:
                else
                      w' \leftarrow w_i/w_{i-1}
22:
                end if
23:
           end if
24:
           Randomly set \bar{\delta}_i \leftarrow \delta_i or \bar{\delta}_i \leftarrow \delta_i + 1 with probabilities w' and 1 - w' respectively
25:
           if A_i \leq \delta_i then
26:
                i \leftarrow i + 1
27:
28:
           else
29:
                break
           end if
30:
31: end while
32: if A_{i_0} \leq \delta_{i_0} then
           k_{FDP} \leftarrow i - 1
33:
34: else
35:
           k_{FDP} \leftarrow 0
36: end if
37: R_{\alpha,\gamma} \leftarrow \{i : \text{the (pre-sorted) } W_i \text{ is in the top } k_{FDP} \text{ ranks and } L_i = 1\}
```

Algorithm A3 GR-SD (adopted from Guo and Romano (2007))

```
Input: • (p_i)_{i=1}^m the list of p-values;
```

- $\alpha \in (0,1)$ the FDP threshold;
- $\gamma \in (0,1)$ for a $1-\gamma$ confidence level;

Output: A discovery list $R_{\alpha,\gamma}$

1: sort the p-values (p_i) in ascending order

b ties are randomly broken

- 2: **for** i = 1, ..., m **do**
- 3: $k_i \leftarrow |\alpha i| + 1$
- 4: $\delta_i \leftarrow F^{-1}[k_i, m-i+1](\gamma)$
- $\triangleright F[\alpha, \beta](\cdot)$ denotes the CDF of a Beta (α, β) RV

- 5: end for
- 6: $k_{GR} \leftarrow \max\{i: \prod_{j=1}^{i} 1_{p_i \leq \delta_i} = 1 \text{ or } i = 0\}$
- 7: $R_{\alpha,\gamma} \leftarrow \{i \in [m] : i \leq k_{GR}\}$

Algorithm A4 RESET

- **Input:** $\{(L_i, W_i, \mathbf{x}_i) : i = 1, ..., m\}$ each hypothesis' (label, winning score, side information);
 - α FDR threshold for the discovery list;
 - s the probability of assigning a decoy to the training set (default: s = 1/2);
 - \bullet f a semi-supervised machine learning model;
 - c_0 an upper bound probability for a true null label $\mathbb{P}(L_i = 1) \leq c_0$ (*i* is a true null);
 - isFDR a boolean which determines whether FDR or FDX control is desired;
 - γ a confidence parameter if FDX control is desired;

Output: A discovery list R

- 1: $I \leftarrow$ a subset of the decoy win indices, $\{i : L_i = -1\}$, determined by independently including each one with probability s
- 2: $L_i \leftarrow -1$ for $i \in I$

3: $\tilde{L}_i \leftarrow 1$ for $i \in J := I^c$

▷ pseudo-targets

4: $(\widetilde{W}_i)_{i=1}^m \leftarrow f\left((W_i, U_i, \widetilde{L}_i)_{i=1}^m\right)$

 \triangleright rescoring using the semi-supervised f

- 5: if isFDR then
- 6: $R \leftarrow \text{SSS}+((\widetilde{W}_i, L_i)_{i \in J}, c = c_e := \frac{c_0}{1-s \cdot (1-c_0)}, \alpha)$

⊳ Selective SegStep+

- 7: else
- 8: $R \leftarrow \text{FDP-SD}((\widetilde{W}_i, L_i)_{i \in J}, c = c_e = \frac{c_0}{1 s \cdot (1 c_0)}, \alpha, \gamma)$

▶ FDP-stepdown

- 9: end if
- 10: return R

B Proofs

B.1 RESET controls the FDR or FDX

By Lemma 1 in the main text, conditional on \mathcal{G} the true null labels among the pseudo-targets are independent ± 1 random variables, though not necessarily identically distributed. From this and either Lemma 1 of Barber and Candès (2015) or Lemma 2 of Lei and Fithian (2018), it can be shown that RESET controls the FDR. On the other hand, FDX control does not immediately follow from existing lemmas; one must separately check that the FDP-SD proof still holds when the true null labels are non-identical.

We therefore introduce a new two-step proof that simultaneously addresses RESET's FDR and FDX control in the non-identical setting. Our approach may be of independent interest, since the extension to the non-identical setting holds for a generic multiple testing procedure. Specifically, we show that any procedure which controls FDR or FDX with true null probabilities $\mathbb{P}(L_i = 1) = c_i$ also controls them whenever $\mathbb{P}(L_i = 1) \leq c_i$. Second, we verify RESET's control in the special case of Lemma 1 where the true null labels are identically distributed conditioned on \mathcal{G} , i.e., $\mathbb{P}(L_i = 1 \mid \mathcal{G}) = c_e$, and then invoke the first step to cover the general case, $\mathbb{P}(L_i = 1 \mid \mathcal{G}) \leq c_e$.

Definition 1. Let $(n_i)_{i=1}^{m_0}$ and $(a_i)_{i=1}^{m_1}$ be subsequences that partition [m]. Let $(c_i)_{i=1}^m$ be a sequence of probabilities in [0,1]. An input template \mathcal{I} is any configuration of the data such that:

- 1. $(H_{n_i})_{i=1}^{m_0}$ are true null hypotheses and $(H_{a_i})_{i=1}^{m_1}$ are false null hypotheses;
- 2. all the scores $(W_i)_{i=1}^m$ as well as the labels $(L_{a_i})_{i=1}^{m_1}$ of the false null hypotheses are fixed;
- 3. conditioned on the false null labels $(L_{a_i})_{i=1}^{m_1}$ and on all the scores $(W_i)_{i=1}^m$ the labels of the true null hypotheses are independent with $P(L_{n_i} = 1) = c_{n_i}$.

Lemma B3. Suppose R is a multiple hypothesis selection procedure (filter) that:

- 1. Accepts as input label-score pairs $(L_i, W_i)_{i=1}^m$;
- 2. Reports only a subset of the target wins $(L_i = 1)$;
- 3. For fixed $(c_i)_{i=1}^m$, R controls the FDR/FDX for any input template \mathcal{I} .

Then R controls the FDR/FDX for a fixed $(c_i^*)_{i=1}^m$ in the above sense (3), where $c_i^* = c_i$ for $i \neq j$ and $c_i^* = 0$.

Proof. Let \mathcal{I}^* be any input template for the sequence $(c_i^*)_{i=1}^m$. Suppose H_j is a false null hypothesis. Then FDR/FDX control trivially follows from the original assumptions since \mathcal{I}^* only depends on $(c_i^*)_{i=1}^m$ only through $(c_{n_i}^*)_{i=1}^{m_0} = (c_{n_i})_{i=1}^{m_0}$. Otherwise, there exists $n_i = j$ for some $i \in [m_0]$. Define \mathcal{I}' to be the input template that is identical to \mathcal{I}^* except that H_j is a false null hypothesis and $L_j := -1$. Again, R controls the FDR/FDX on \mathcal{I}' by the original assumptions since \mathcal{I}' depends on $(c_i^*)_{i=1}^m$ only through $(c_{n_i}^*)_{i=1,n_i\neq j}^{m_0} = (c_{n_i})_{i=1,n_i\neq j}^{m_0}$. Notably, since for \mathcal{I}^* we have $P(L_j = 1) = 0$ and since we set $L_j := -1$ for \mathcal{I}' , from the perspective of R the two input templates are identical. Moreover, because R cannot report decoy wins, the FDP in its list of discoveries is the same for \mathcal{I}^* and \mathcal{I}' , hence R also controls the FDR/FDX on \mathcal{I}^* with $(c_i^*)_{i=1}^m$.

Lemma B4. Under the assumptions of Lemma B3, R controls the FDR/FDX for a fixed $(c_i^*)_{i=1}^m$ where $c_i^* = c_i$ for $i \neq j$ and $c_j^* \in [0, c_j]$.

Proof. If $c_j = 0$, then the Lemma is trivial. Otherwise, consider any input template \mathcal{I}^* with $c_j^* \in [0, c_j]$. Define \mathcal{I}_1 to be the input template that is identical to \mathcal{I}^* except that c_j^* is set to c_j . Similarly, define \mathcal{I}_2 to be the input template that is identical to \mathcal{I}^* except that c_j^* is set to 0. We can generate data from \mathcal{I}^* by stochastically sampling from the two related templates \mathcal{I}_1 and \mathcal{I}_2 . First, independently of everything else we draw a value B from a Bernoulli distribution with $P(B=1) = c/c_j$. Next, if B=1 we sample from \mathcal{I}_1 , otherwise we sample from \mathcal{I}_2 .

Note that R controls the FDR/FDX on samples generated according to the \mathcal{I}_1 template by the original assumptions, and it similarly controls the FDR/FDX on \mathcal{I}_2 by Lemma B3. It therefore follows from the law of total expectation/probability that S controls the FDR/FDX on the template \mathcal{I}^* .

Corollary 5. Under the assumptions of Lemma B3, R controls the FDR/FDX for a fixed $(c_i^*)_{i=1}^m$ where $c_j^* \in [0, c_j]$ for all $j \in [m]$.

Proof. The result follows by induction on m using Lemma B4.

We are now ready to prove that RESET controls the FDR or FDX where we first address the special case where the true null labels are identically distributed conditioned on \mathcal{G} . We use Corollary 5 to extend our proof to the general case.

Proof of Theorem 1. For each $i \in J$ where $J = \{i \in [m] : \tilde{L}_i = 1\}$, we assign a one-bit p-value:

$$\tilde{p}_i = \begin{cases} c_e & L_i = +1 \\ 1 & L_i = -1. \end{cases}$$

Recall that the scores \widetilde{W} are themselves a function of \mathcal{G} and clearly each one bit p-value \widetilde{p}_i is a function of the labels L_i . It follows from Lemma 1 of the main text that conditioned on the scores \widetilde{W} and the one-bit p-values of the false nulls, the one-bit p-values of the true nulls $(\widetilde{p}_i)_{i\in J\cap N}$ are independent with $\mathbb{P}(\widetilde{p}_i \leq c_e) = \mathbb{P}(L_i = 1) \leq c_e$, i.e., they stochastically dominate the uniform distribution. Suppose the labels are identically distributed so that $\mathbb{P}(\widetilde{p}_i \leq c_e) = \mathbb{P}(L_i = 1) = c_e$ for $i \in J \cap N$. Then the conditions of Theorem 3 in Barber and Candès (2015) hold and applying, as RESET does, Selective SeqStep+ to the labels $(L_i)_{i\in J}$ and scores $(W_i)_{i\in J}$ with $c=c_e$ controls the FDR at level α . Now suppose the labels are non-identical so that $\mathbb{P}(L_i = 1) \leq c_e$ for $i \in J \cap N$. Selective SeqStep+ is a procedure that satisfies the conditions of Lemma B3 and so it follows from Corollary 5 that RESET also controls the FDR at level α .

Remark 1. It is worth noting that the original formulation of Selective SeqStep+ in Barber and Candès (2015) uses one-bit p-values instead of labels. However, these are equivalent since we identify the event $\{\tilde{p}_i = c_e\}$ with $\{L_i = 1\}$ and $\{\tilde{p}_i = 1\}$ with $\{L_i = -1\}$.

Proof of Theorem 2. It follows from Lemma 1 of the main text that conditioned on the scores \widetilde{W} and the labels of the false nulls, the labels of the true nulls $(L_i)_{i\in J\cap N}$ are independent with with $\mathbb{P}(L_i=1)\leq c_e$. Suppose the labels are identically distributed so that $\mathbb{P}(L_i=1)=c_e$ for $i\in J\cap N$. Then this satisfies the assumption of FDP-SD with $c=\lambda=c_e$ (see Section 4 of Luo et al. (2023)) and applying, as RESET does, FDP-SD to the labels $(L_i)_{i\in J}$ and scores $(W_i)_{i\in J}$ controls the FDX at α with confidence $1-\gamma$. Now suppose the labels are non-identical so that $\mathbb{P}(L_i=1)\leq c_e$ for

 $i \in J \cap N$. FDP-SD is a procedure that satisfies the conditions of Lemma B3 and so it follows from Corollary 5 that RESET also controls the FDX at level α with confidence $1 - \gamma$.

B.2 Proof of Lemma 2 in the main text

We provide a proof of Lemma 2 which is essentially the same as in Chao and Fithian (2021) but has been adapted using our notation.

Proof of Lemma 2. By Assumption 4, since the pairs (L_i, W_i) are determined by p_i (and vice versa), the null pairs $(L_i, W_i)_{i \in N}$ are independent conditioned on the side information \mathbf{x} and the false null pairs $(L_i, W_i)_{i \notin N}$. Since each L_i only possibly depends on W_i , the labels $(L_i)_{i \in N}$ are independent if we further condition on all of W, the side information \mathbf{x} , and the labels $(L_i)_{i \notin N}$. This proves the first part of Assumption 3.

Suppose \mathbf{x} and $(p_i)_{i \notin N}$ are fixed in the remaining probability statements. Then for $i \in N$, since L_i only possibly depends on W_i ,

$$\mathbb{P}(L_{i} = 1 \mid W_{i}) = \frac{\mathbb{P}(p_{i} \in [0, a) \mid W_{i})}{\mathbb{P}(p_{i} \in [0, a) \mid W_{i}) + \mathbb{P}(p_{i} \in (b_{1}, b_{2}] \mid W_{i})} \\
\leq \frac{\mathbb{P}(p_{i} \in [0, a) \mid W_{i})}{\mathbb{P}(p_{i} \in [0, a) \mid W_{i}) + \mathbb{P}(p_{i} \in [0, a) \mid W_{i}) \cdot \frac{b_{2} - b_{1}}{a}} \\
= \frac{a}{a + b_{2} - b_{1}} \\
= c_{0},$$

where the first line follows since the denominator sums to 1, and the second line follows from the non-decreasing property as explained next.

First, note that the non-decreasing density property from Assumption 4 implies that for a true null p-value p_i $(i \in N)$ and a measurable $B \subseteq [0, a)$

$$\mathbb{P}(p_i \in B) \le \frac{a}{b_2 - b_1} \cdot \mathbb{P}(p_i \in q(B)), \tag{5}$$

where q denotes the inverse transformation of the mirroring that maps p-values in $(b_1, b_2]$ onto [0, a), that is $q(p) := b_2 - \frac{b_2 - b_1}{a} \cdot p$.

Let $A \subseteq \mathbb{R}$ be measurable and let $B \subseteq [0, a)$ be such that $\{W_i \in A\} = \{p_i \in B\} \cup \{p_i \in q(B)\}$. Then,

$$\int_{W_{i} \in A} 1_{p_{i} \in [0,a)} d\mathbb{P} = \int 1_{\{p_{i} \in [0,a) \cap B\}} d\mathbb{P} = \mathbb{P}(p_{i} \in B)$$

$$\leq \frac{a}{b_{2} - b_{1}} \mathbb{P}(p_{i} \in q(B))$$

$$= \frac{a}{b_{2} - b_{1}} \int 1_{\{p_{i} \in (b_{1},b_{2}] \cap q(B)\}} d\mathbb{P}$$

$$= \frac{a}{b_{2} - b_{1}} \int_{W_{i} \in A} 1_{p_{i} \in (b_{1},b_{2}]} d\mathbb{P},$$

Since A was arbitrary, it follows that:

$$\mathbb{P}(p_i \in [0, a) \mid W_i) \le \frac{a}{b_2 - b_1} \mathbb{P}(p_i \in (b_1, b_2] \mid W_i).$$

Remark 2. As part of AdaPT's assumptions, Lei and Fithian (2018) directly assume Equation (5), which they call mirror-conservatism. Lemma 2 is therefore true under a broader class of true null p-values that satisfy mirror-conservatism, not just those that are non-decreasing as prescribed by AdaPTg's assumptions (Chao and Fithian (2021)) and our Assumption 4.

C Supplementary Methods

C.1 Summary of methods

- 1. AdaFDR: AdaFDR splits the pairs $(p_i, \mathbf{x}_i)_{i=1}^m$ into two folds. For each fold, the method fits a mixture model to optimally rescore the hypotheses, and the model is then applied to the other fold where a list of discoveries is obtained. The two list of discoveries are joined together and then reported. AdaFDR's mixture model is a composition of Gaussian components to model local 'bumps' of genuine signals (false nulls) within the data plus an additional component that captures the monotonic relationship between the side information and the signals.
- 2. AdaPT: AdaPT works by iteratively pruning a candidate set of hypotheses $\hat{\mathcal{S}}_t$, similar to Adaptive Knockoffs, which was derived from it. At each iteration, AdaPT fits a two-group mixture model on a strict subset of information: the p-values outside $\hat{\mathcal{S}}_t$, the masked p-values in \hat{S}_t given by $(p_i \wedge (1-p_i))_{i \in \hat{S}_t}$ where $1-p_i$ is referred to as the *mirrored* p-value, the side information \mathbf{x} , as well as $\#\{i \in \hat{\mathcal{S}}_t : p_i > 1/2\}$ and $\#\{i \in \hat{\mathcal{S}}_t : p_i < 1/2\}$. It then removes the hypothesis from $\hat{\mathcal{S}}_t$ that is deemed most likely to be a true null based on the fitted model. To fit the mixture model, the EM algorithm is used. The M-step of the EM algorithm results in a regression problem which allows the user to flexibly use the regression method of their choice. The authors considered a generalized additive model (GAM), a generalized linear model (GLM), and a generalized linear model with L_1 regularization (GLMnet). If we identify each p-value $p_i > 1/2$ with a label $L_i = -1$ and each p-value $p_i < 1/2$ with a label $L_i = 1$, then AdaPT terminates this pruning procedure at step τ when the estimated FDR, as in Equation (3) of the main text, is $\leq \alpha$. The rationale is that for true null hypotheses, the p-values are usually uniformly distributed, so $\#\{i \in \hat{\mathcal{S}}_t : L_i = -1\}$ estimates the number of true null hypotheses with positive labels, $\#\{i \in \hat{\mathcal{S}}_t : L_i = 1\}$. It then reports the remaining positively labelled hypotheses in $\hat{\mathcal{S}}_{\tau}$. Note, AdaPT and its variants do not use labels explicitly — we introduce those here for notational convenience.
- 3. AdaPT_g: AdaPT_g generalizes AdaPT by constructing asymmetric regions to define the positive and negative labels. For example, the p-values $p_i \in (0.3, 0.9)$ can be identified with a

label $L_i = -1$ and the p-values $p_i < 0.3$ can be identified with a label $L_i = 1$. One advantage of defining these asymmetric regions, is to avoid overestimating the number of true null hypotheses in cases where their p-values are not uniformly distributed and there is a concentration of true null p-values near 1. Subsequently, the estimated FDR needs to be adjusted to account for the fact that we expect twice as many true null p-values with negative labels than positive labels.

- 4. AdaPT-GMM_g: AdaPT-GMM_g replaces the two group mixture model in AdaPT_g for a Gaussian mixture model (GMM). Similar to AdaPT/AdaPT_g, it also allows the user to choose from a collection of regression methods to fit the model at the M-step of the EM algorithm.
- 5. ZAP-asymp: Lastly, ZAP-asymp directly fits a beta mixture model to the data but is only able to offer asymptotic FDR control. Importantly, ZAP-asymp can operate directly on the test statistic instead of just the corresponding p-values to rerank the hypotheses. This is particularly advantageous for two-sided tests because the test statistic is mapped to its p-value in a non-bijective manner, losing information regarding the sign of the original test statistic along the way. Note that AdaPT-GMM_g can also operate on test statistics, but in this paper, we focus on the p-value information.

C.2 Further implementation details of RESET

C.2.1 Handling hypotheses with a score of zero

RESET throws out the hypotheses with undefined labels, i.e., those hypotheses with $W_i = 0$. We try to recover some of this information in the following way. If the proportion of zero-scoring hypotheses is at least 0.01, then for each hypothesis with $W_i \neq 0$, we identify the k-nearest neighbours in terms of the side information (zero-scoring hypotheses included). Then we define an extra side information variable as the number of zero-scoring hypotheses among these identified neighbours (we used k = 20).

C.2.2 Handling noisy side information

To reduce the effect of 'noisy' side information that is unable to distinguish between true and false nulls, we implement an initial side information selection procedure. Specifically, we use a generalized additive model to fit a smoothing spline using $W \cdot \tilde{L}$ as the response against each user-provided side information variable one at a time. We use tryCatch in case the smoothing spline fails, in which case we fit the response directly to the side information variable, that is, we use a linear fit. Again, we try to make use of some of the zero-scoring hypotheses setting $W \cdot \tilde{L} = 0$ in these cases. We keep only the side information variables with sufficiently small p-values in the fitted model (p < 0.01).

C.2.3 Positive set for training

Not all the pseudo-targets need to be included in the initial positive set in Step (i). After all, we expect many of the pseudo-targets to be true nulls. Hence, to improve the performance of RESET, we consider the following strategy. For each feature in (W, \mathbf{x}) , reorder the hypotheses according to that feature, and apply SSS to the pseudo labels \tilde{L} at the FDR level α . Then select the feature that maximizes the number of pseudo discoveries. Then using the chosen feature, we define the positive set as those pseudo-targets discovered at α_0 , again using SSS with the pseudo labels \tilde{L} (we used $\alpha_0 = 50\%$ throughout). Usually the score is selected, but in some cases the side information is highly informative and is selected instead. Users interested in a small FDR level, like $\alpha = 1\%$, could probably benefit from reducing α_0 to further improve the performance, and in particular the speed, of RESET (though as we mentioned, we kept $\alpha_0 = 50\%$ across the board).

To ensure that the positive set is always large enough, we increase α_0 by increments of 0.01 until the positive set reaches min_positive = 50 or until all the pseudo-targets are in the positive set. This is applied to both the initial positive set and the second round of training.

C.2.4 Handling dependent data

Real data often exhibits dependency to some degree, failing to satisfy Assumption 3, which guarantees RESET's finite sample FDR/FDX control. To overcome this challenge, we implement the

following two modifications when applied to p-value based data in RESET Ensemble and its variants.

The first modification is in Step (ii). For each fold $k \in [K]$, we replace each score W_i from the negative set in the training folds, $[K] \setminus \{k\}$, with scores drawn i.i.d from $|\Phi^{-1}((b_2 - p_i) \cdot \frac{a}{b_2 - b_1})|$ where $p_i \sim U[b_1, b_2]$. In other words, we replace the scores of the negative set for those obtained from uniform p-values before each training phase.

Note that we only modify the p-values of the negative set in the training folds: all the p-values in the test folds remain unchanged. This reduces any leakage of information from the training folds into the test folds and in the final stage when the estimating decoys are used to report a list of discoveries.

The following second modification is motivated by the observation that the Random Forest is particularly sensitive to local dependencies. Specifically, if there are several hypotheses that exhibit essentially the same p-value and side information, then the same observation is essentially split across all folds. The flexibility of Random Forest enables it to overfit to these local regions of hypotheses and significantly overshoot the FDR threshold.

In the second modification we apply k-nearest neighbours to the side information of the set of training decoys. Next, we sum over the squared differences between each training decoy's score W_i and its k-neighbours, denoted as ss_{obs} . We perform a bootstrap-like procedure in which we shuffle the scores of the training decoys B = 1000 times and subsequently compute the sum of squares as previously described for each shuffle, producing $(ss_i)_{i=1}^B$. We compute a one-sided p-value by calculating the fraction of bootstrapped sum-of-squares smaller than ss_{obs} . If the p-value is ≤ 0.01 , the user is notified that the data may exhibit local dependency, and we remove the Random Forest from the ensemble of classification algorithms. If RESET RF is implemented and the p-value is ≤ 0.01 , then RESET RF switches to RESET NN with default parameters.

Our detection method above compares how close the scores are, through ss_{obs} , versus the collection of $(ss_i)_{i=1}^B$ in which the scores are no longer dependent on the side information. Thus a p-value that is ≤ 0.01 is likely to catch data exhibiting local dependency. To make the k-nearest neighbours more efficient, and to be certain that the procedure is only applied to true null hypotheses, we consider only the training decoys that have a small enough mirrored p-value, i.e.,

 $(b_2 - p_i) \cdot \frac{a}{b_2 - b_1} \le 0.1$ and we restrict number of neighbours to $k = 100 \wedge \lceil 0.01 \cdot m \rceil$, where m is the number of considered hypotheses used in RESET.

We demonstrate the robustness of our modifications in Section 6.3 in which we show that RESET Ensemble appears to empirically control the FDR using dependent p-values, along with our analysis of real data in Section E.2. In cases when the data satisfies Assumption 3, our above modifications do not violate finite sample FDR/FDX control.

C.2.5 Other technical details

We point out some additional minor details regarding our implementation of RESET. We use the randomForest package, nnet and mgcv to implement the random forest, two-layer neural network and generalized additive model in R, respectively. We used the default parameters for the random forest except with 1000 trees, the default parameters for the two-layer neural network and the default parameters for the generalized additive model (except we use drop.intercept = TRUE). If the number of side information variables used by RESET is ≤ 3 , a smoothing spline is fitted with mgcv::s otherwise a natural cubic spline is fitted using 5 degrees of freedom with splines::ns on each side information variable separately (for computational efficiency). If GAM fails to fit, we used tryCatch to remove the smooth terms and therefore becoming just a linear model. Some real datasets contain p-values that are 'zero'. Hence when we calculate $W_i = |\Phi^{-1}(p_i)|$ for such p-values, we obtain Inf in R. We replace instances of Inf for the maximum real-valued score in the dataset. Unless otherwise stated, we used the same default settings of RESET for all simulated and real data experiments, which includes all of the heuristics described in this section (Section C.2).

C.3 Competition-based multiple testing: the knockoff filter

The competition framework was popularized in the statistics community in the context of variable selection, where the goal is to identify relevant variables from $\{X_i : i = 1, ..., p\}$ that are conditionally associated with a response y. The procedure that achieves this while controlling the FDR is called the *knockoff filter*, which begins by pairing each variable X_i with an artificial variable \tilde{X}_i , called a *knockoff*. In this paper, we consider the *model-X* version of the knockoff filter (Candès et al. (2018)) which makes the following assumptions. First, the joint distribution of the variables,

X, is assumed to be known. Second, each observation $(X_{i,1}, \ldots, X_{i,p}, y_i)$ is sampled *i.i.d.* from the joint distribution F_{XY} . Because X is random and its distribution known, the knockoffs \tilde{X} are also constructed randomly subject to the following conditions:

- 1. The joint distribution of $\hat{X} := [X, \tilde{X}]$ is the same if we swap a subset of the variables and their corresponding knockoffs, i.e., $\hat{X} \circ \Pi \stackrel{d}{=} \hat{X}$, where Π is a permutation that swaps the subset of variable indices for their corresponding knockoff indices.
- 2. We construct \tilde{X} independently of y by only looking at X, i.e., $\tilde{X} \perp y \mid X$.

Once the knockoffs have been constructed, each variable is given a user-defined score $W_i([X, \tilde{X}], y) \in \mathbb{R}$ and a label $L_i([X, \tilde{X}], y) \in \{\pm 1\}$. As in the competition framework described in Section 2, the idea is that the label L_i indicates whether the variable X_i or the knockoff \tilde{X}_i has greater evidence for being relevant to the model, and the score W_i indicates by how much. Commonly, the score and label are combined by setting $sign(W_i) = L_i$; however, given our presentation of RESET, it is instructive to separate them.

In this paper, we consider the Lasso Coefficient Difference (LCD) score, which is the difference in the magnitude of the coefficients of the Lasso regression (Tibshirani (1996)). Specifically, cross-validation is used to determine the λ penalty when regressing on the augmented design matrix $[X, \tilde{X}]$. We denote the absolute values of the Lasso(λ)-fitted coefficients as Z_i for the variables and \tilde{Z}_i for the knockoffs. The scores and labels are then defined as

$$W_i := |Z_i - \tilde{Z}_i|, \quad L_i := sign(Z_i - \tilde{Z}_i), \tag{6}$$

where hypotheses with zero scores are thrown out.

C.4 Further implementation details of Adaptive Knockoffs

There were some small differences between the implementations in the adaptiveKnockoff package in R and the code used in the original manuscript. Accordingly, we used the updated package version. We also fixed a minor bug, which pruned the candidate set \hat{S}_t before checking the estimated FDR is $\leq \alpha$ — possibly missing out on a marginally larger discovery list. There are several

parameters that may be set before applying the Adaptive Knockoff filters, e.g., the initial proportion of hypotheses revealed, reveal_prop. We used the same parameter settings in Simulation 1 here as in Simulation 1 in Ren and Candès (2023) (which uses one-dimensional side information), and the same parameter settings in Simulations 2-4 here as Simulation 2 in Ren and Candès (2023) (which uses two-dimensional side information or more).

In the application to peptide detection, the primary score W can be negative. Since Adaptive Knockoffs encodes the labels L by using the sign of the scores W, we shifted our peptide scores so that the minimum score was zero in those cases. For AdaKO EM, any peptide score $\leq 10^{-3}$ was subsequently assigned a zero score. Finally we used, reveal_prop = 10% which reveals the hypotheses that are less than or equal to the 10% of positive scoring hypotheses (which is the same setting used by the simulations). All other parameters were default.

C.5 Simulation details for the competition setting

C.5.1 Simulation 1: Linear model with one-dimensional side information

Our first simulation is based on Simulation 1 of Ren and Candès (2023). Specifically, n = 1000 independent observations from the joint data distribution of (X,Y) are generated by drawing X from a hidden markov model (HMM) with p = 900 variables and $Y|X \sim \mathcal{N}(X\beta,I)$ (linear model). The β 's are selected in the following way. Let k denote the number of nonzero β 's. Then k indices from $\{1,2,\ldots,2k\}$ are sampled without replacement, each with probability proportional to $1/i^2$. The k chosen indices are the nonzero β 's and are assigned a value of $\pm 3.5/\sqrt{n}$, where the signs are chosen i.i.d. uniformly. We consider $k \in \{50,150,300\}$ while the original simulation only considers k = 150. We generate HMM knockoffs from Sesia et al. (2019). Each hypothesis is supported by the side information $\mathbf{x}_i = i$, which should help in detecting the nonzero β 's, because smaller values of i are more likely to correspond to a nonzero β_i .

We generated 100 independent datasets each consisting of drawing n observations as described above. The original simulation in Ren and Candès (2023) sampled the β 's once and fixed them across the 100 datasets. Here we redrew the β 's for each dataset so that we may average our results over a range of models, as we noticed that all the methods exhibited significant variability between

the draws.

C.5.2 Simulation 2: Linear model with two-dimensional side information

In a second simulation, we considered a larger linear model where n = 2000 observations are taken from the joint distribution (X, Y) as described in Section C.5.1, with p = 1800. Accordingly, we also adjusted the number of false nulls to $k \in \{150, 300, 450\}$. Note that unlike the previous simulation, it is not relevant how the k variable indices are selected from $\{1, 2, ..., p\}$. Each hypothesis is equipped with the following two-dimensional side information. For the ith hypothesis, we draw a pair of observations \mathbf{x}_i from a bivariate normal $\mathcal{N}(\boldsymbol{\mu}, I)$ with $\boldsymbol{\mu} = (0, 0)$ for a true null hypothesis and $\boldsymbol{\mu} = \pm (2, 2)$ for a false null hypothesis, where the signs are chosen i.i.d. uniformly. We generated 20 independent datasets of this larger simulation instead of 100, where each involved drawing those n observations, β coefficients, and side information variables.

C.5.3 Simulation 3: Logistic model with two-dimensional side information

Next, we consider Simulation 2 by Ren and Candès (2023). They generate n = 1000 observations with p = 1600 variables sampled from the joint data distribution of (X, Y), where X is distributed according to a multivariate normal distribution and $Y|X \sim \text{Bernoulli}\left(e^{\beta \cdot X}/\left(1 + e^{\beta \cdot X}\right)\right)$ is a logistic model (see Ren and Candès (2023) for further details). Each hypothesis' side information is a unique pair of values $\mathbf{x}_i = (\mathbf{x}_{i1}, \mathbf{x}_{i2})$ from the lattice $[-20, 19] \times [-20, 19] \subseteq \mathbb{Z}^2$. The nonzero β 's are chosen according to the position of $(\mathbf{x}_{i1}, \mathbf{x}_{i2})$ in the lattice. An image of the nonzero β 's is given in Figure C9. Each nonzero β is set to $\pm 25/\sqrt{n}$, where the signs are chosen *i.i.d.* uniformly. We generate approximate SDP Gaussian knockoffs as described in Candès et al. (2018).

We generated 100 independent datasets drawing n observations as above in each but for 2 of those AdaKO EM failed with an error so we used only 98 of the datasets. The original simulation in Ren and Candès (2023) sampled the sign of the β 's once, fixing them across the 100 datasets. Instead, we redraw the sign of the β 's in each of the 98 datasets since we found that the results of all the methods significantly varied with those draws.

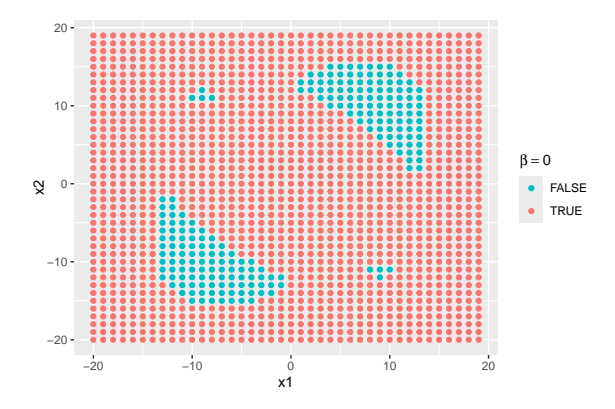


Figure C9: Location of nonzero β 's according to the pair of values (x, y) in the lattice. The same image is given in Ren and Candès (2023).

C.5.4 Simulation 4: Large p and n and 3-d side information

Finally, in the last simulation, n=10K observations with p=10K variables and k=0.15p relevant variables are drawn from the joint data distribution (X,Y) exactly as described in Simulation 1. Each variable is equipped with the following three-dimensional side information. The first k variables are randomly assigned a value drawn from $i \in \{1, \ldots, 2k\}$ taken without replacement and having probability proportional to $1/i^2$. The remaining p-k variables are uniquely assigned to one of the remaining values from $i \in \{1, 2, \ldots, p\}$ uniformly at random. Overall, the final assignment is a permutation of the integers in $\{1, \ldots, p\}$, subject to the constraint that the first k variables take values exclusively from $\{1, \ldots, 2k\}$. We expect most of the nonzero β 's to have small values of i, but the effect of the random assignment makes the resulting side information variable less informative than in Simulation 1, as depicted in Figure C10. This process is repeated three times, thus associating three side information variables with each hypothesis, which taken together, should be reasonably informative. We generated 5 independent samples, drawing the n observations, β coefficients, and side information in each.

C.6 Competition-based multiple testing: peptide detection

Competition-based multiple testing was first established in the proteomics community where the goal is to infer which proteins, i.e., long chains of amino acids, are present in a biological sample (Elias and Gygi (2007)). Direct protein detection is challenging, and so a bottom-up approach is taken where the proteins are digested into small chains of amino acids, called *peptides*, and the

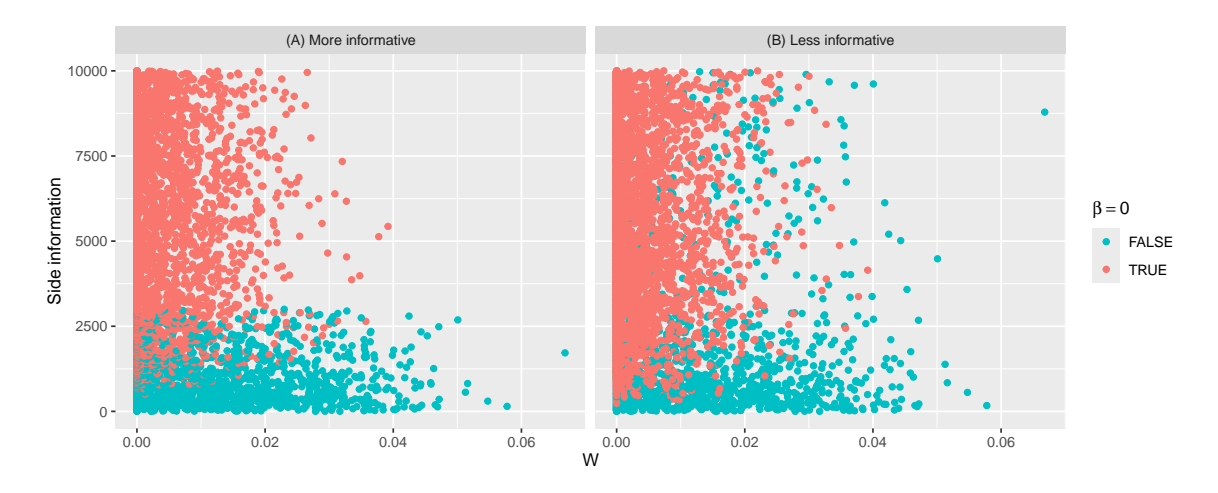


Figure C10: Scatterplot of each hypothesis according to the LCD score denoted as W (x-axis) and side information variable (y-axis). Each hypothesis is coloured according to whether it is a true (red) or false null hypothesis (blue). In (A), the side information variable is the index of the hypothesis in Simulation 1 (Section C.5.1). In (B), we use one of the three side information variables as described in Simulation 4 (Section C.5.4).

objective is to identify these peptides instead. Then, a process called *liquid chromatography tandem* mass spectrometry (LC-MS/MS) is used in which a first round of mass spectrometry isolates each sample peptide and reports the abundance or intensity of each sample peptide. In a second round of mass spectrometry, each sample peptide that reports a high enough intensity is selected and further fragmented. The intensity of each fragment is then reported in a corresponding fragmentation spectrum. Each such spectrum can be thought of as a fingerprint of the peptide that generated the spectrum, allowing us to hypothesize which peptides are present in the sample.

This is done by searching each spectrum against a database of candidate peptides called targets to find the spectrum's optimal peptide-spectrum match (PSM), along with a score indicating the strength of the match. Unfortunately, due to the incomplete nature of the database and the noise associated with generating the spectra, the PSM can be incorrect. Hence, we wish to employ a testing procedure for each null hypothesis H_i that 'the *i*th target is not present in the sample'. In order to decide which null hypotheses to reject, we pair each target peptide with a decoy peptide that is generated by randomly shuffling or reversing the target peptide's sequence. Accordingly, a second search is performed for each spectrum against the database of decoys to obtain a second PSM and associated score, and only the highest scoring PSM out of the two is retained.

The search phase described above is dictated by a range of user-specified parameters. The most common configuration of these parameters correspond to two broad types of searches, namely

narrow and open searches, which we consider in this paper. Briefly a 'narrow' search, which is the default search mode, only searches each spectrum in the spectrum file against peptides in the target-decoy database that have a theoretical mass within a small tolerance of the mass of the sample peptide that generated the experimental spectrum. On the other hand, an 'open' search makes this mass-tolerance larger so that a spectrum may match with a peptide with a completely different mass. This is desirable at times, since sample peptides can undergo post-translational modifications which modify the mass of the peptide so it no longer matches its theoretical mass. However, when searching in an 'open' mode, the modified spectrum may still be correctly matched.

The same database peptide, target or decoy, may be matched multiple times with different scores, or have no match at all. Hence, we associate with H_i the score Z_i , defined as the maximum scoring PSM associated with the *i*th target peptide, and by its design the higher the score, the more likely H_i is false, i.e., the peptide is in the sample. Similarly, we define the null drawn \tilde{Z}_i as the maximum scoring PSM associated to the *i*th target's corresponding decoy peptide. Target or decoy peptides that have no matching spectra are assigned a score of $-\infty$. Finally, we obtain a winning score $W_i = Z_i \vee \tilde{Z}_i$ and a label L_i indicating whether the winning score was from the *i*th target or its decoy (where ties are randomly broken). Peptides with a winning score of $-\infty$, indicating that neither the target nor its paired decoy have a matching spectra, are thrown out. Finally, a competition-based multiple testing procedure like SSS+ or FDP-SD may be applied to these scores and labels (Nesvizhskii (2010)).

C.7 Further implementation details of the AdaPT methods

We applied AdaPT using the adaptMT package in R. In Simulations 5 and 6, we used the same settings considered by Lei and Fithian (2018), i.e., we used AdaPT GAM in Simulation 5 and AdaPT GLMnet in Simulation 6 with the same parameters. Moreover, we considered AdaPT GLMnet in Simulation 5 with the same settings from Simulation 6, demonstrating the importance of selecting the correct working model. In Simulations 7 and 8, we used the same settings as Simulation 5. In the real datasets looked at by Zhang et al. (2019), we used AdaPT GAM to fit a natural cubic spline using splines::ns with 5 degrees of freedom (knots chosen by default) on each side information variable. The use of natural cubic splines is a suggested option from the

package documentation. There was an exception to this for the GTEx datasets, which flagged an error when we tried to apply the spline basis transformation on the 'chromatin state of the SNP'. In this case, we applied no transformation to the affected side information variable. Zhang et al. mention that they employed a "5-degree for each dimension", but it is not clear to us if they mean the degree of the piece-wise polynomials that make the spline, or the degrees of freedom of the spline. In the latter case, it is not clear how the knots are chosen, or how they overcame the error associated with the 'chromatin state of the SNP'. Regardless, our results using AdaPT appear to be essentially the same. Moreover, Zhang et al. omit the application of AdaPT to the two fMRI datasets on account of the categorical side information variable used in these datasets. However, Chao and Fithian appear to still apply AdaPT_g without problem, and so analogously we applied AdaPT as well. Lastly, in the gene-drug response data, we followed the same implementation by Lei and Fithian (2018), which used AdaPT GLM and a collection of candidate side information transformations using splines::ns with degrees of freedom ranging from 6 to 10.

C.8 Further implementation details of the AdaPT_g methods

We downloaded AdaPT_g from the repository https://github.com/patrickrchao/adaptMT which has all the same implementations as AdaPT while offering the ability to define asymmetric regions for mirroring the p-values. Accordingly, we followed the same implementation details as the previous section used by AdaPT and set the so-called 'masking parameters' as default.

C.9 Further implementation details of AdaPT-GMM $_{\rm g}$

We downloaded AdaPT-GMM_g from the repository https://github.com/patrickrchao/AdaPTGMM. In Simulations 5, 7 and 8, we used the GAM filter (model_type = 'mgcv') to fit a smoothing spline using mgcv::s on the side information for the M-Step of the EM algorithm. In Simulation 6, we used a generalized linear model filter with regularization (model_type = 'glmnet') applied directly to the side information variables. For the real datasets used by Zhang et al. (2019), we used the exact same implementation as Chao et al. from the file https://github.com/patrickrchao/AdaPTGMM_Experiments/blob/main/AdaFDR_experiments/run_all_exp.R. In the gene-drug response data, since only one-dimensional side information is used, we copied the parameters selected from the

previous real datasets that also considered just one-dimensional side information.

C.10 Further implementation details of ZAP

We used the default parameters of zap_asymp from the ZAP package https://github.com/dmhleung/ zap. In all simulations and real data experiments, we considered a natural cubic spline basis expansion on each side information variable with six degrees of freedom using splines::ns. This choice was based on their own analysis on two of the real datasets that we consider here, Airway and Bottomly. The exception was in Simulation 6, where we directly used all 100 side information variables rather than applying a spline basis expansion on each of them. ZAP requires explicit test-statistics, specifically z-scores, as input. In Simulations 5, 7 and 8, we used the test statistics as input. Since the p-values are obtained from a one-sided test, there is a one-to-one correspondence between the p-value information and test statistic information. Thus our comparisons in Simulations 5, 7, and 8, are still effectively based on the p-values as we addressed in Section 3.1. In Simulation 6, explicit z-score test statistics were not generated by the simulation. Hence, we used the inverse normal CDF Φ^{-1} to convert the p-values to a z-score test statistic. In the real data experiments, instead of directly using the $\Phi^{-1}(p_i)$, we converted the p-values to z-values using the transformation $\pm \Phi^{-1}(p_i/2)$ on each p-value p_i where the signs are chosen i.i.d. uniformly. Otherwise, applying the transformation $\Phi^{-1}(p_i)$ to true null p-values with a non-decreasing density, or a spike near 1, will produce consistently large z-scores and will be incorrectly discovered by ZAP as an artefact of the data transformation.

C.11 Further implementation details of AdaFDR

We applied AdaFDR using the method.adafdr_test function from the AdaFDR package https://github.com/martinjzhang/adafdr. We note that installation of the package required setting up a separate conda environment so that we could install an older version of Python (v3.6.13). This was because recent versions of Python do not support PyTorch v1.4.0, a requirement of the AdaFDR package setup.py file.

We used the exact same parameters in the vignettes https://github.com/martinjzhang/ AdaFDRpaper/tree/master/vignettes to implement AdaFDR on the 10 datasets that Zhang et al. look at. Interestingly, the two fMRI datasets only consider the Brodmann label as the side information. We tried using all the available side information, but the statistical power was worse (data not shown). In the gene-drug response data, we used AdaFDR with fast_mode = False. This is in accordance to the discussion from their paper that the fast version of AdaFDR is recommended when few discoveries are expected or if the number of hypotheses is small (which is not the case for both of the gene-drug response datasets). For the same reasons, we used AdaFDR with fast_mode = True on Simulation 5 when the number of hypotheses was small, and fast_mode = False on Simulations 7 and 8 when the number of hypotheses were large.

C.12 Simulation details for p-value setting

C.12.1 Simulation 6

Simulation 6 in Section 6.2.2 models "noisy" side information since only the first 2 of the 100 draws are used to distinguish between the true and false null hypotheses. Each p-value p_i is drawn *i.i.d.* from a two-group beta mixture model, where the true nulls have a uniform distribution and the false nulls have an alternative beta distribution. Specifically, the beta mixture model is given by:

$$f(p_i \mid \mathbf{x}_i) = 1 - \pi(\mathbf{x}_i) + \pi(\mathbf{x}_i) \cdot h(p_i; \mu(\mathbf{x}_i)), \quad h(p_i; \mu(\mathbf{x}_i)) = \left(\frac{1}{\mu(\mathbf{x}_i)} p_i^{\frac{1}{\mu(\mathbf{x}_i)} - 1}\right), \tag{7}$$

where $\mathbf{x}_i \in [0, 1]^{100}$ denotes the side information of the *i*th hypothesis, $\pi(\mathbf{x}_i)$ denotes proportion of the false nulls in the mixture, h denotes the false null distribution of Beta $(1/\mu(\mathbf{x}_i), 1)$. The $\pi(\mathbf{x}_i)$'s and $\mu(\mathbf{x}_i)$'s are determined by the following relationships with the 100-dimensional side information:

$$\log\left(\frac{\pi}{1-\pi}\right) = \theta_0 + \mathbf{x}_i^T \theta, \quad \mu_i = \max\{\mathbf{x}_i^T \beta, 1\},$$

where $\theta = (3, 3, 0, ..., 0) \in \mathbb{R}^{100}$, $\beta = (2, 2, 0, ..., 0) \in \mathbb{R}^{100}$ and θ_0 is chosen to satisfy $\frac{1}{m} \sum_i \pi(\mathbf{x}_i) = 0.3$. Clearly, only the first two values in $\mathbf{x}_i \in [0, 1]^{100}$ contribute to the beta mixture model, as intended. We generated 100 independent datasets, where in each we drew the 2000 p-values as described.

C.12.2 Simulation 7 (false null probability)

The *i*th hypothesis is randomly identified as a false null dependent on its side information \mathbf{x}_i) with probability (Figure C11)

$$\pi_i := \pi(\mathbf{x}_i) := 0.1 \cdot \sum_{j=0}^2 w_j \cdot f_j(\mathbf{x}_i),$$

where $(w_0, w_1, w_2) = (0.5, 0.25, 0.25)$, f_1 and f_2 are normal densities with parameters $(\mu_1, \sigma_1) = (0.25, 0.05)$ and $(\mu_2, \sigma_2) = (0.75, 0.05)$ respectively, truncated between 0 and 1 and normalized such that $\int_{[0,1]} f_1 dx = \int_{[0,1]} f_2 dx = 1$, and $f_0(x) := a \cdot \exp(ax)/(\exp(a) - 1)$ where a = 0.5.

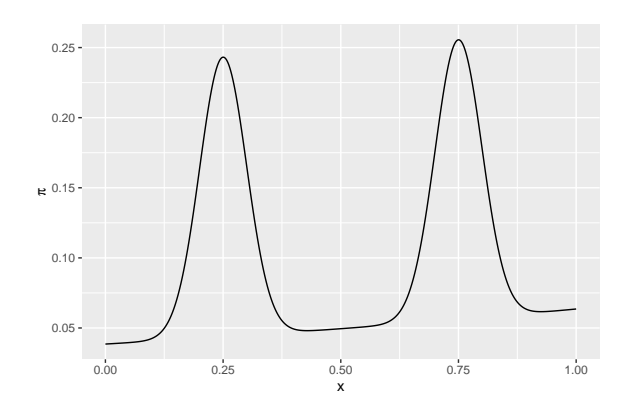


Figure C11: The probabilities of a hypothesis being a false null, π , as a function of the hypothesis' side information, \mathbf{x} .

C.13 Computer specifications for computation times

Computation times were calculated using an M1 Mac Studio with 20-core CPU and 128GB RAM.

C.14 Estimating the computation times of Adaptive Knockoffs

Running Adaptive Knockoffs (AdaKO) on each of the HEK293 and PRIDE-20 spectrum files is impractical. We therefore resorted to estimate its runtime, which requires dealing with two challenges. The first is that the runtime of each iteration of AdaKO, where it determines which hypothesis to reveal next, varies with the number of remaining hypotheses. The second is that we cannot precisely predict the number of iterations AdaKO will take.

Addressing the second challenge first, we note that AdaKO starts by revealing the label of any hypothesis H_i for which $W_i \leq q_{0.1}^*$, where q_c^* is the c-quantile of all positive scoring hypotheses. Let

m' be the number of remaining hypotheses after this initial reveal. The number of iterations that AdaKO will make before stopping is then $m' - \ell$, where ℓ is the number of hypotheses (target or decoy peptides) that remain when it stops. We can estimate ℓ with $\hat{\ell}$, the number of target and decoy peptides that score above the 1% FDR cutoff using RESET Ensemble. Thus we estimate the number of AdaKO iterations by $m' - \hat{\ell}$.

To estimate the runtime of each iteration we resorted to taking k measurements. Indeed, for each $i \in \{1, ..., k\}$, we revealed the labels of any hypotheses H_i for which $W_i \leq q_{(0.1\cdot i)}^*$ and determined the time it took for AdaKO to reveal the next label. We chose k to be the largest positive integer such that the number of remaining labels, after revealing the labels L_i for which $W_i \leq q_{(0.1\cdot k)}^*$, is still more than $\hat{\ell}$. Thus, we obtain the runtime of k single iterations that are evenly spaced, starting from AdaKO's first iteration and ending at approximately AdaKO's last iteration before it terminates with $\hat{\ell}$ remaining hypotheses. Next, we computed \bar{t}_k , the average of those k measurements. Thus our overall estimate is:

$$\bar{t}_k \cdot (m' - \hat{\ell}).$$

In the analysis of the PRIDE-20 data in Section E.2, we considered 10 repeated applications of RESET Ensemble, varying RESET Ensemble's internal seed. In this case, we define $\hat{\ell}$ as the average of the number of winning target and decoy peptides above the cutoff over each application.

C.15 Method-related figures

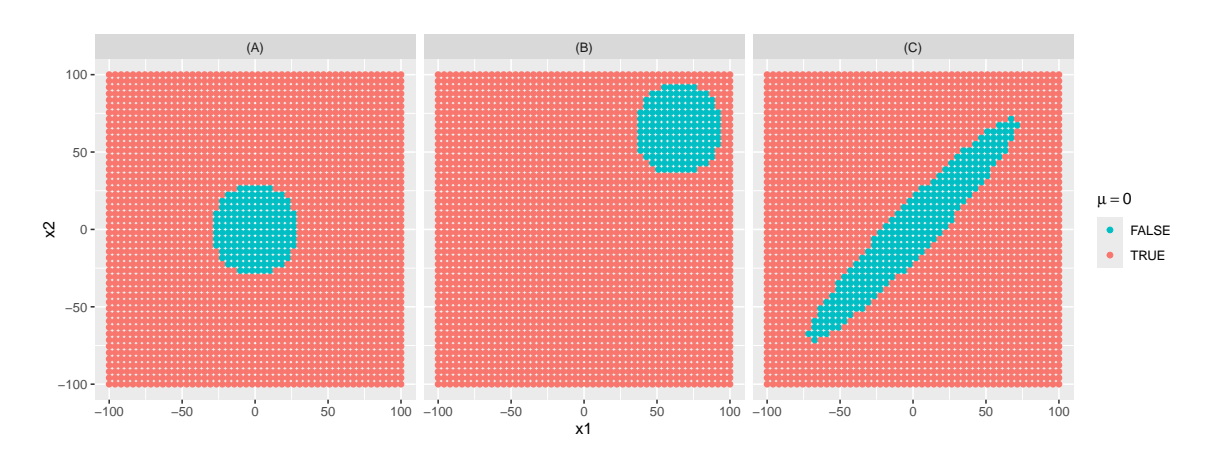


Figure C12: Location of false null hypotheses according to the pair of values $(\mathbf{x}_{i1}, \mathbf{x}_{i2})$ in the square $[-100, 100] \times [-100, 100]$. The same figure is given in Lei and Fithian (2018).

D Data preparation

D.1 Data preparation and searching with HEK293 data

We downloaded the human proteome (UP000005640, downloaded on 2023/09/23 from UniProt) and prepared a target peptide database along with 5 randomly shuffled decoy peptide databases using Tide-index within the Crux Toolkit v4.1.6809338 (Park et al. (2008); Kertesz-Farkas et al. (2023)) with all options set to default. An output containing the target and decoy peptide pairs are conveniently provided using the --peptide-list T option in Tide-index. Each of the RAW 24 HEK293 spectrum files (Chick et al. (2015)) were converted to mzML format using MSConvert 3.0.22314 with the vendor peak-picking filter using the default settings. For each of the 5 decoy databases, we performed a 'narrow' search on each spectrum from the combined 24 mzML spectrum files against the combined target-decoy peptide database using Tide-search (Diament and Noble (2011)), using the options --top-match 1 --auto-precursor-window warn --auto-mz-bin-width warn --concat T. The resulting search files were then converted to so-called pin files using the make-pin function in Crux. Each row in the pin files correspond to the optimal peptide-spectrum match (PSM) for each spectrum, the primary score for quantifying this match, called XCorr scores, and a collection of auxiliary information regarding the PSM.

Side Information	Description		
deltCn	The difference between the XCorr score of the two top ranked PSMs with		
	respect to the combined database, divided by maximum of the top PSM XCorr		
	score and 1		
PepLen	The length of the matched peptide, in residues		
Charge	The charge of the precursor ion (ranging from $+1$ to $+5$)		
lnNumSP	The natural logarithm of the number of database peptides within the specified		
	precursor range		
dm	The difference between the calculated and observed mass		
absdM	The absolute value of the difference between the calculated and observed mass		

Table D3: List of described side information used by HEK293 data. The list of side information used by RESET and Adaptive Knockoffs in the HEK293 data, adapted from https://crux.ms/file-formats/features.html. Note that the Charge state is represented as a one-hot vector, where we left out a Charge state of +1 (due to linearity, since the one-hot vector sums to one).

We constructed the target and decoy peptide scores, Z_i and \tilde{Z}_i respectively, according to our description in Section C.6 using the XCorr score as the PSM scoring function. Subsequently we record the winning score $W_i = Z_i \vee \tilde{Z}_i$ along with the label $L_i = sign(Z_i - \tilde{Z}_i)$. In the case of ties

 $(Z_i = \tilde{Z}_i)$, we randomly set L_i to be +1 or -1 with equal probability. To each pair (W_i, L_i) we attribute the side information defined as the auxiliary information \mathbf{x}_i of the underlying PSM that had the XCorr score of W_i . In the case there is more than one PSM with the same XCorr score of W_i , we randomly select one of the target PSMs if $L_i = +1$ or one of the decoy PSMs if $L_i = -1$. The side information that was subsequently used by RESET and Adaptive Knockoffs is given in Table D3.

D.2 Data preparation and searching with PRIDE-20 data

We followed the preparation and searching outlined in Freestone et al. (2024). The only difference is that we used an updated version of the Crux toolkit. We provide the following brief description for the reader's convenience. Twenty spectrum files and protein databases from separate projects, referred to as the PRIDE-20 dataset, were downloaded (see Table 2 in Freestone et al. (2024)). Tide-index was used to prepare the target peptide database along with 10 randomly shuffled decoy peptide databases for each of the 20 spectrum files. Tide-search was used to search each spectrum file against the 10 combined target-decoy databases using two modes: 'narrow' and 'open' search options as outlined in Freestone et al. (2024). The search files were then converted to pin files using the make-pin function in Crux and subsequently filtered for the top 1 (the optimal) peptide-spectrum match for each spectrum.

For each spectrum file and search type, we obtained the triples (L, W, \mathbf{x}) in the following way. For each spectrum file that had no modifications (we explain this in more detail next), we proceeded essentially in the same way as in Section D.1. That is, for each peptide in the pin file, we define Z_i (if a target peptide) or \tilde{Z}_i (if a decoy peptide) as the maximum Tailor score of all the PSMs associated to the target peptide (Sulimov and Kertész-Farkas (2020)). Here we are using the more sensitive Tailor score and relegate the XCorr score as one of the side information variables. Then we compete each target and its corresponding paired decoy in the same way as Section D.1, to obtain the triple (L_i, W_i, \mathbf{x}_i) where the side information \mathbf{x}_i is obtained from the auxiliary information of the underlying PSM that had the Tailor score of W_i . A description of the side information used is given in Table D4.

We next consider spectrum files that were searched with variable modifications (---auto-

Side Information	Description		
deltLCn	The difference between the XCorr score of the top scoring PSM and the		
	fifth/last ranked PSM with respect to the combined database, divided by the		
	maximum of the top PSM's XCorr score and 1		
deltCn	The difference between the XCorr score of the two top ranked PSMs with		
	respect to the combined database, divided by maximum of the top PSM XCorr		
	score and 1		
Xcorr	The SEQUEST cross-correlation PSM score		
PepLen	The length of the matched peptide, in residues		
Charge	The charge of the precursor ion (ranging from $+1$ to $+5$)		
lnNumSP	The natural logarithm of the number of database peptides within the specified		
	precursor range		
dm	The difference between the calculated and observed mass		
absdM	The absolute value of the difference between the calculated and observed mass		

Table D4: List of described side information used by PRIDE-20 data. The list of side information used by RESET and Adaptive Knockoffs in the PRIDE-20 data, adapted from https://crux.ms/file-formats/features.html. Note that the Charge state is represented as a one-hot vector, where we left out a Charge state of +1 (due to linearity, since the one-hot vector sums to one). XCorr is used as side information since we define W in terms of Tailor scores here instead.

modifications T). Here we need to make a slight adjustment to account for some dependency within the data. Specifically, using variable modifications creates several 'copies' of the peptides in the target-decoy database that are distinguished only by slight alterations to the mass of some of the amino acids. As an example, PEPTIDE may generate the following 'copies': PE[16]PTIDE, PEPTIDE[16] and PE[16]PTIDE[16], where [16] indicates an increase of 16 Daltons to the amino acid on the left. Consequently, the scores of all these peptides are usually correlated: if one of these is scored high, than often they all are. Hence in order to satisfy Assumption 3, we follow the protocol outlined in Freestone et al. (2024). That is, we identify all the copies as being the same peptide, 'PEPTIDE', with each of the variable modifications ignored. Then we proceed with the same steps as the above paragraph, by determining the maximum score associated with PEPTIDE and recording it as Z_i (or \tilde{Z}_i if it is a decoy). We define the labels, winning scores and side information in the same way to obtain our triplets (L, W, \mathbf{x}) .

Due to runtime considerations, we used 13 of the spectrum files to assess Adaptive Knockoff's power as described in Section 5.2.2 of the manuscript (each resulting in < 33K PSMs), and only one of the 10 target-decoy databases. To fairly compare with Adaptive Knockoffs, we used the same target-decoy databases for RESET ensemble. All 20 spectrum files and all 10 target-decoy databases for each spectrum file were used in comparing RESET Ensemble's FDX control with

D.3 Description of real data with p-values

We provide the following description of each dataset used in Section 6.4 in the main text and in Section F.3. The following three RNA-seq datasets, the proteomics dataset, the two microbiome datasets, the two fMRI datasets, and the two eQTL datasets were downloaded from https://github.com/patrickrchao/AdaPTGMM_Experiments/tree/main/AdaFDR_experiments/data_files. The last gene-drug response data was obtained from the adaptMT package.

- Three RNA-seq datasets (Airway (Himes et al. (2014)), Bottomly (Bottomly et al. (2011)), Pasilla (Brooks et al. (2011))): The goal is to identify genes that are associated with varying gene expression levels in response to a change of conditions. In the Airway data, the differential expression analysis is conducted in response to a drug, dexamethasone; in the Bottomly data, the analysis is conducted between two mouse strains; and in the Pasilla data, the analysis is conducted between normal and so-called 'Pasilla knockdown' conditions (Huber and Reyes). In all cases the side information consists of the log-normalized gene expression read counts.
- A proteomics dataset (Proteomics (Dephoure and Gygi (2012))): The goal is to identify proteins that have different protein abundances when treated with rapamycin versus DMSO in yeast cells. Each protein consists of side information equal to the natural log of the number of peptides belonging to the protein that were 'quantified' in all six samples.
- Two microbiome datasets (Microbiome Enigma Ph and Microbiome Enigma Al (Smith et al. (2015); Korthauer et al. (2019))): The goal is to identify microbiome organisms, recorded as OTUs (Operational Taxonomic Units), that are associated with certain conditions (pH and Al). Each hypothesis (OTU) is equipped with a two-dimensional side information the ubiquity, which is defined as the percentage of samples detected with the OTU, and the mean nonzero abundance, which is defined as the average abundance of each OTU across the samples in which it was detected.

- Two fMRI datasets (Auditory and Imagination (Tabelow and Polzehl (2011))): The goal is to identify voxels that are activated in response to different stimuli. In the first dataset, a single individual received auditory stimulus and in the second dataset, a single individual was instructed to imagine playing tennis. Each hypothesis (voxel) is equipped with four dimensional side information: the spatial position of the voxel (in three dimensions) and a categorical variable with the Brodmann label (Brodmann (1909)), which is used to delineate different areas of the brain with different functions.
- Two eQTL datasets (Subcutaneous and Omentum (Consortium et al. (2015); Consortium (2020))): The goal is to identify single nucleotide polymorphisms (SNPs) that are associated with changes in gene expression levels. Such an association is referred to as an expression quantitative trait locus (eQTL). Each hypothesis (SNP) is equipped with the following four side information variables: (1) the distance between the SNP and the gene transcription's start site (TSS), (2) the log gene expression level, (3) the alternative allele frequency (AAF) of the SNP and (4) the chromatin state of the SNP.
- Gene-drug response data (Estrogen (Davis and Meltzer (2007); Li and Barber (2017))): The goal is to identify genes that are differentially expressed in response to a low-dosage estrogen treatment applied to breast cancer cells. Each hypothesis (gene) is assigned a 'rank' that was generated using an analysis of the gene expression levels in response to (1) a high-dosage estrogen treatment and (2) a medium-dosage estrogen treatment. Here, the ranks are in terms of the strength of association between the expression level of each gene and the level of dosage in (1) and (2). Thus, we can analyse the data twice, once for each side information variable based on (1) and (2).

D.4 Preparation of data with p-values

All pairs of p-values and side information from the above datasets were used to report a list of discoveries using each p-value based method with the following exceptions. In the RNA-seq datasets, Airway, Bottomly and Pasilla, there exists 'spikes' of high p-values (Figure D1, top row). These spikes are associated with genes with low log-normalized read count. Hence, removing all

genes with log-normalized read count less than zero — whose information content is questionable anyhow — also eliminated those undesirable spikes (Figure D1 bottom row). The number of genes removed is given in Table D5.

Dataset	# of genes removed	% of genes removed
Airway	10616	32%
Bottomly	2203	16%
Pasila	1575	13%

Table D5: The number and percentage of genes removed from the RNA-seq datasets.

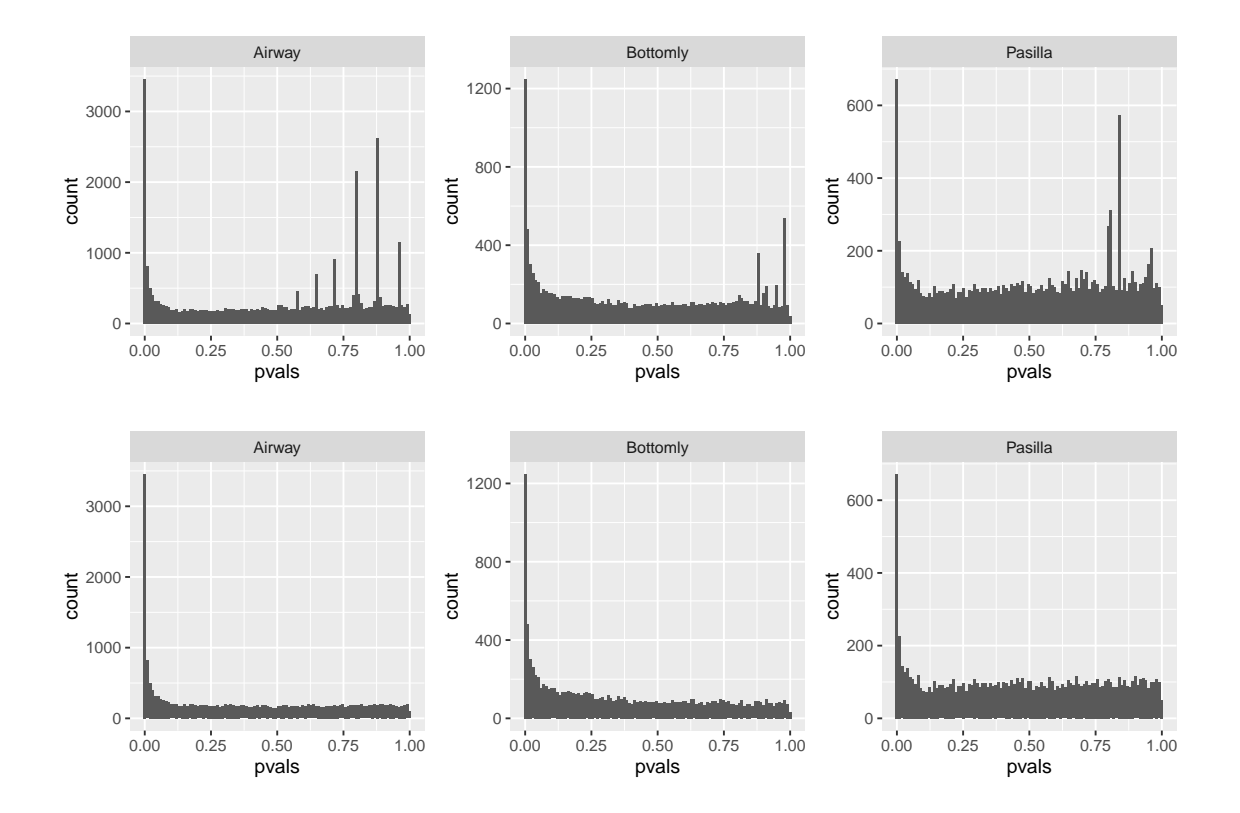


Figure D1: Histograms of p-values in the RNA-seq data before and after removal of genes with negative lognormalized read count. Top row: the original histograms of the p-values. Bottom row: the corresponding histograms after the removal of genes with low read counts.

E Supplementary results

E.1 Further comparisons between RESET and AdaKO in simulations

For each simulation and FDR threshold in Figure 1 of the main text, we determined the maximum power across all RESET and AdaKO methods and computed the relative power of each method to this maximum. The resulting relative powers are reported as boxplots in Figure E1A, giving an indication of the performance of each method across the simulations as a whole. Additional plots showing the performance of each method in each separate simulation are given in Figures E2 (power) and E3 (estimated FDR).

While in Figure E2 we often find a version of AdaKO that is more powerful, or at least comparable to RESET Ensemble, this varies between the versions. On the other hand, RESET Ensemble's performance is consistent across these simulations, and overall typically achieves the highest relative power when the results are aggregated. Interestingly, RESET NN seems to be marginally more powerful than RESET Ensemble. While this may be the case, we still recommend RESET Ensemble as the default approach to alleviate the burden of selecting any single classification algorithm, as for example, RESET Ensemble appears to perform marginally better in the p-value setting (see Figure 6 of the main text).

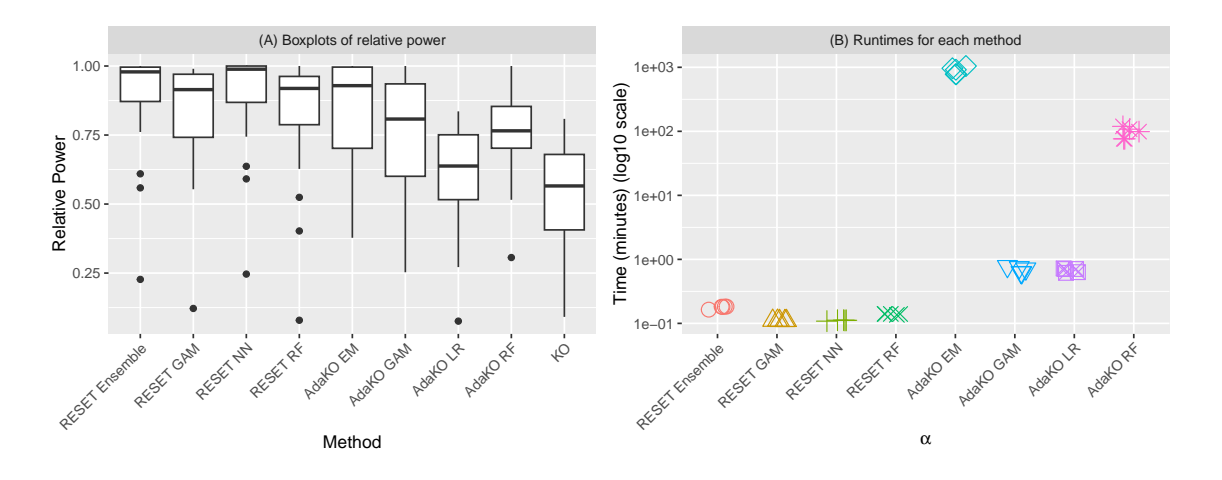


Figure E1: **Relative power and runtimes for each method.** (A) Each boxplot describes the relative power for each method, computed across the combination of simulations and FDR thresholds in Figure 1. (B) The log10 runtimes of each method applied at the 5% FDR level for 5 runs of Simulation 4. For readability, the points are jittered in the horizontal direction.

One advantage of RESET is its computational speed. Indeed, our implementation of RESET, as

described in Section 4.4 of the main text, has many steps that can be parallelized: the r evaluations of each classification algorithm on the K folds can all be done in parallel using multiple cores. In contrast, Adaptive Knockoffs must iteratively apply a classification algorithm for every nonzero scoring hypothesis in the candidate set \hat{S}_t until the estimated FDR is $\leq \alpha$, or all hypotheses are revealed. Figure E1B demonstrates this advantage showing the (log10) runtimes of RESET (using 20 CPUs) and of Adaptive Knockoffs at the 5% FDR level across 5 runs of Simulation 4. We find that each version of RESET is significantly faster than each version of Adaptive Knockoffs. RESET Ensemble is around 10^3 to 10^4 times faster than AdaKO EM, 10^2 to 10^3 times faster than AdaKO RF, and about 3-5 times faster than AdaKO LR and AdaKO GAM.

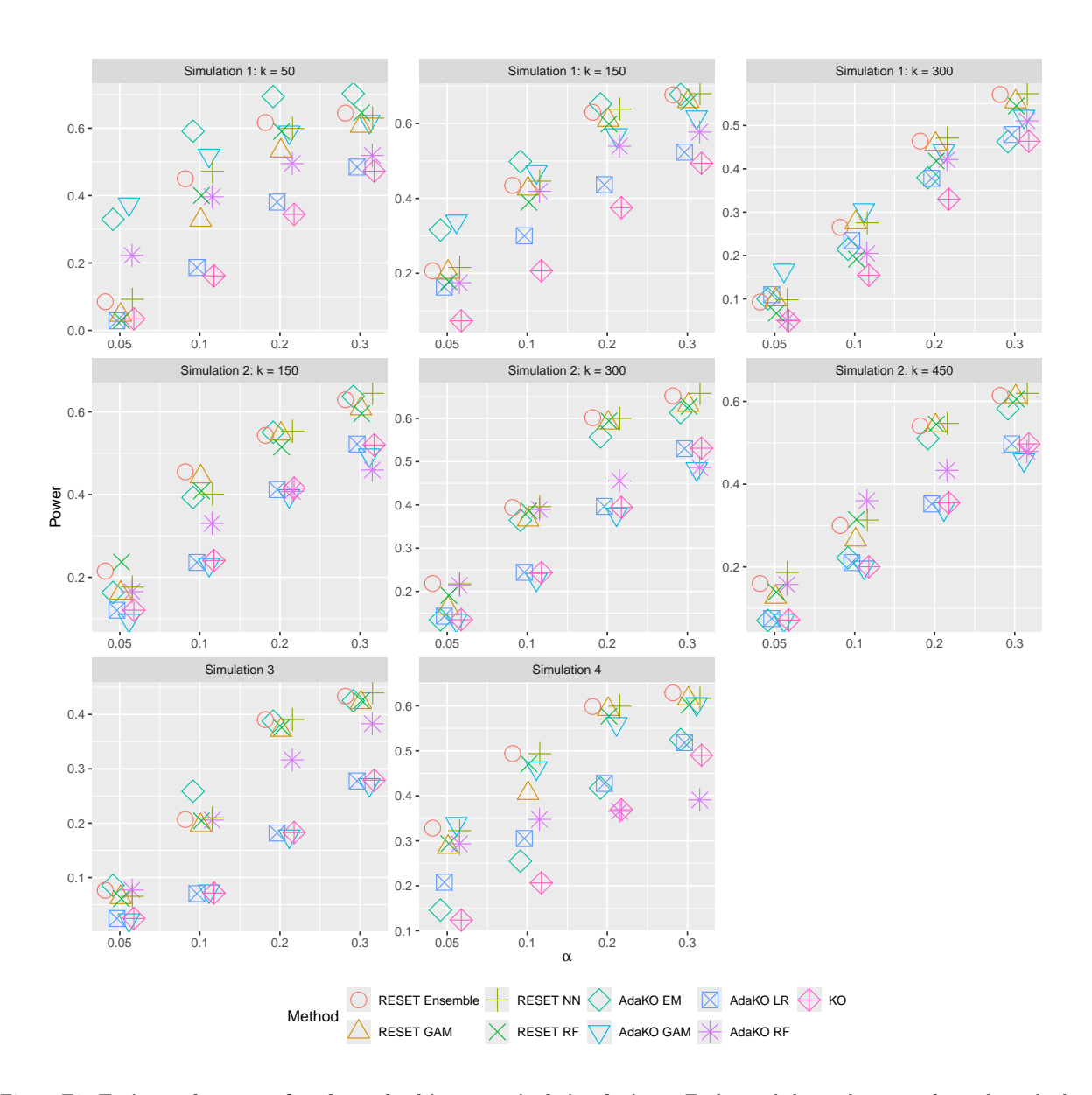


Figure E2: Estimated power of each method in numerical simulations. Each panel shows the power for each method at FDR thresholds ranging from 5% to 30%. The first row corresponds to Simulation 1 with three values of $k \in \{50, 150, 300\}$, the second row corresponds to Simulation 2 with three values of $k \in \{150, 300, 450\}$, and the last row corresponds to Simulations 3 and 4. For readability, the points are jittered in the horizontal direction. A description of the AdaKO methods and KO can be found in Section 2.

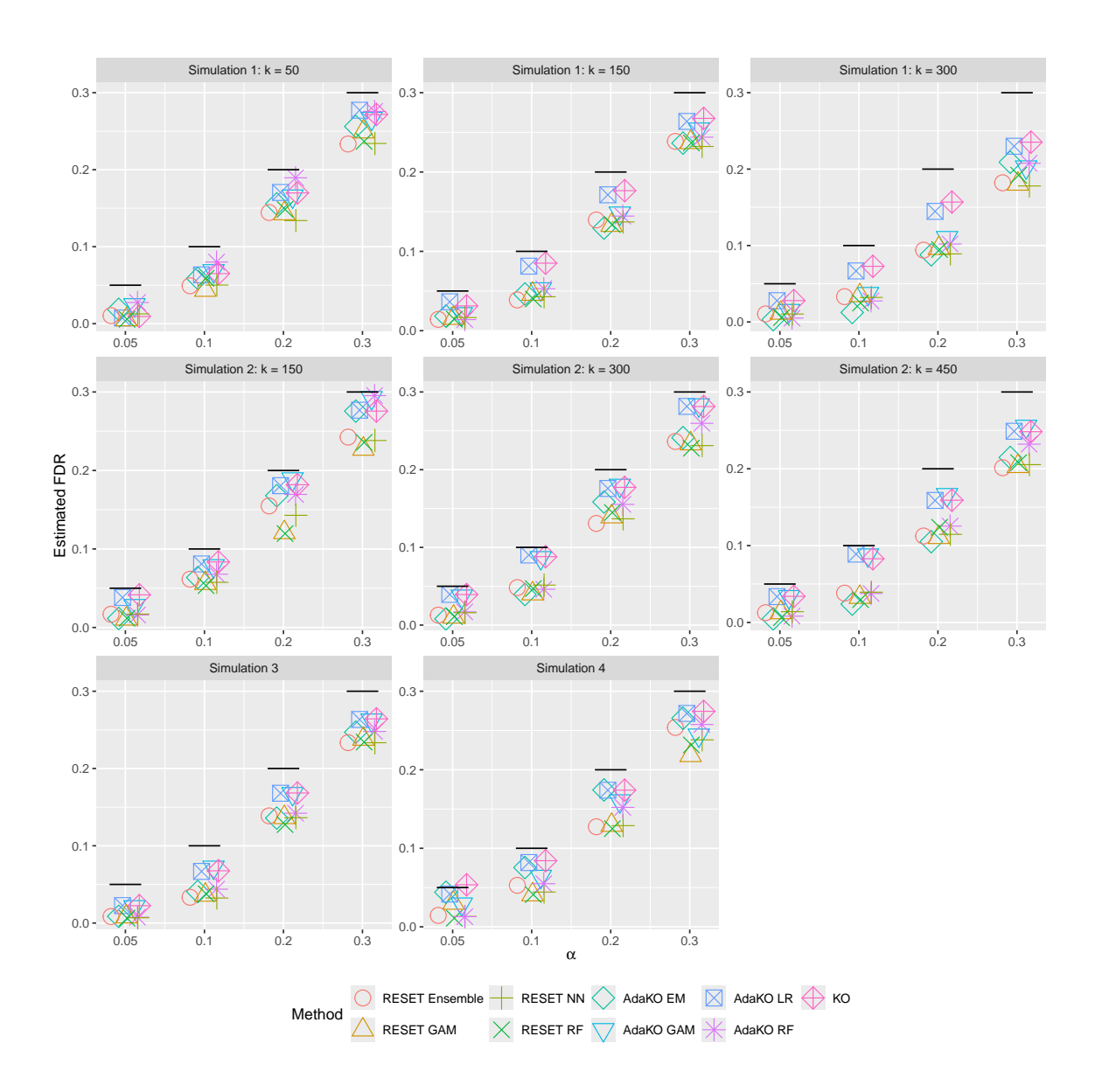


Figure E3: Estimated FDR of each method in numerical simulations. Each panel shows the estimated FDR for each method at FDR thresholds ranging from 5% to 30%. The estimated FDR is calculated as the proportion of irrelevant variables in the discovery list, averaged over the runs. The first row corresponds to Simulation 1 with three values of $k \in \{50, 150, 300\}$, the second row corresponds to Simulation 2 with three values of $k \in \{150, 300, 450\}$, and the last row corresponds to Simulations 3 and 4. For readability, the points are jittered in the horizontal direction.

E.2 Comparison of AdaKO RF and RESET Ensemble using PRIDE data

We looked at the performance of RESET Ensemble versus AdaKO RF because in this setup it was the most powerful implementation of Adaptive Knockoffs. Due to the computational constraints of AdaKO RF, we focused on the results using a narrow search. In Figure E4A, the left boxplot displays the average number of discoveries by RESET Ensemble, divided by the number of discoveries by AdaKO RF using thirteen of the PRIDE-20 spectrum files. In six of the thirteen PRIDE spectrum files, we found RESET Ensemble to be the superior method, while in the remaining seven spectrum files, AdaKO RF produced the same or more discoveries. In one dataset, AdaKO RF discovered 1,217 peptides — approximately an 11% increase over the average of 1,084 peptides discovered by RESET Ensemble.

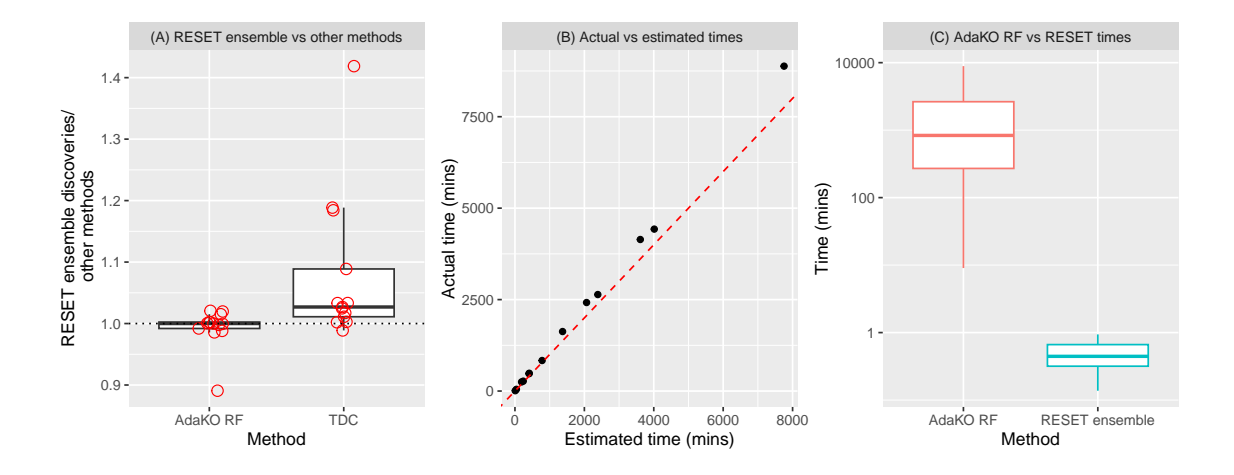


Figure E4: Comparison of RESET Ensemble and AdaKO RF. For each of the 13 PRIDE datasets, we computed the average number of discoveries using 10 applications of RESET Ensemble, varying RESET's internal seed. The left panel shows a boxplot of those RESET Ensemble averages divided by the number of discoveries using AdaKO RF (left boxplot) and TDC (right boxplot) where each circle corresponds to one of the 13 smaller PRIDE-20 datasets. In the centre panel, we compare the estimated and actual runtimes for AdaKO RF. Lastly, in the right panel, we compare the actual runtimes of RESET Ensemble and AdaKO RF (in log10 scale) on the same 13 PRIDE-20 datasets.

We also assessed the computational times of AdaKO RF in Figure E4B, using both the actual and estimated runtimes as outlined in Section C.14. Reassuringly, our estimated times were less than the actual times taken by AdaKO RF to complete. Although we find that, when analysing these smaller spectrum sets, AdaKO RF is the most powerful method of Adaptive Knockoffs, and it is competitive to RESET Ensemble power-wise, it is again clear that AdaKO RF is generally too slow with some runtimes exceeding multiple days even for these small datasets. In fact, on the dataset where AdaKO RF outperforms RESET Ensemble by about 11%, it takes 3.07 days for

Table E1: The average number of (HEK293) discoveries while controlling the FDX. The average number of discoveries reported for RESET Ensemble and FDP-SD on the combined HEK293 spectrum files at different confidence values $1 - \gamma = 0.5, 0.8, 0.9$ and an FDP threshold of 1%. The averages are taken over 5 applications of each method, once for each of the 5 combined target-decoy databases.

	Confidence $1 - \gamma$		
Method	0.5	0.8	0.9
RESET Ensemble	82930	82677	82508
FDP-SD	75977	75450	75255

AdaKO RF to discover its peptides while RESET Ensemble takes about half a minute to complete. Figure E4C shows that in the worst cases, RESET takes roughly 1 minute while AdaKO RF takes over 6 days. The issue of runtimes is especially problematic considering the fact that multiple spectrum files are often analysed jointly, as in our HEK293 analysis in Section 5.2.1.

E.3 FDX control in mass spectrometry data

We evaluated RESET Ensemble's FDX control using the HEK293 and all twenty PRIDE-20 spectrum files (see Sections D.1 and D.2 for data preparation and search settings). As in Section 5.2.1, the joint HEK293 spectrum files were searched against 5 distinct target-decoy databases, where each target-decoy database was generated by concatenating the target database to a decoy database consisting of shuffled target peptides. Similarly, each PRIDE-20 spectrum file was searched against 10 distinct target-decoy databases. We used the coinflip version of FDP-SD (Luo et al. (2023)), which provides a uniform increase in the number of discoveries (at the cost of some randomness in the discovery list, see Supplementary Algorithm A2). Our results using RESET Ensemble and FDP-SD are given in Table E1 and Figure E5.

RESET Ensemble delivers on average approximately 9-10% more HEK293 discoveries than FDP-SD across all confidence levels (Table E1). The picture is somewhat murkier when considering the PRIDE-20 datasets: while RESET Ensemble appears to be generally more powerful (Figure E5, zoomed-in right panel), it fails to make any discoveries at high confidence levels in a few datasets (Figure E5, left panel). Upon a closer look, the numbers of discoveries made by FDP-SD in these datasets are relatively small, with the largest average number of discoveries among these datasets being 417. When the number of discoveries is expected to be small and the confidence parameter is high, RESET may yield less power, even if the side information is reasonably informative — a

phenomenon we dwell on in Section F.4.

RESET Ensemble advantage over FDP-SD is clearer when applying the two procedures to open as opposed to narrow searches. As discussed in Section D.2, an open search allows for the detection of peptides whose masses have been altered by *post-translational modifications* (PTMs). In this setting, side information variables such as dm, which records the mass difference between the peptide and the spectrum, can be highly informative given that some differences will correspond to masses of common PTMs. Thus, it is not surprising that RESET, which can take advantage of such side information, improves on FDP-SD even further across all confidence levels in this context.

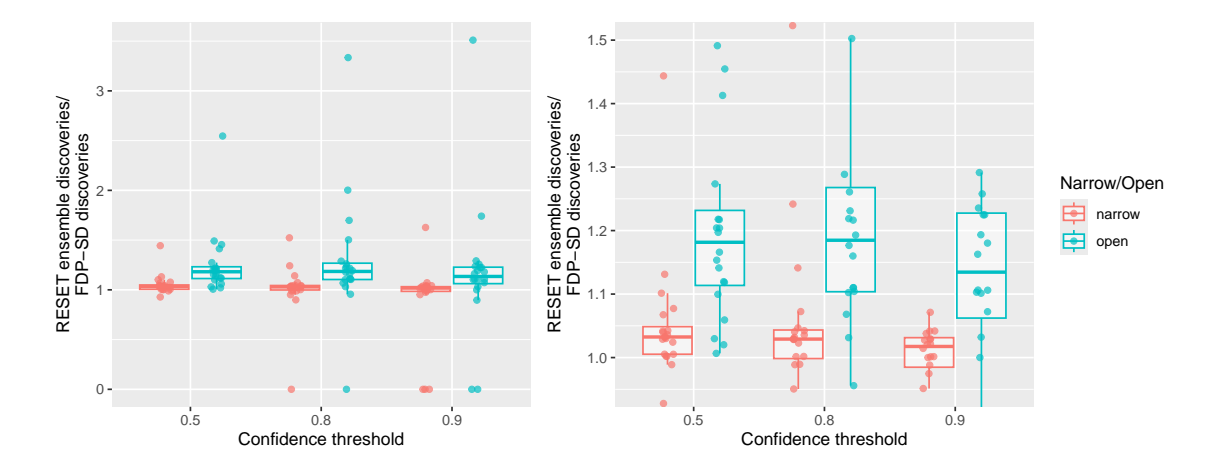


Figure E5: Comparison of RESET Ensemble and FDP-SD. The left panel shows boxplots of the average number of discoveries using RESET divided by the average number of discoveries using FDP-SD (the right panel is just a 'zoomed-in' version). We used all twenty PRIDE-20 datasets at an $\alpha=1\%$ FDP threshold and varying confidence parameters with both narrow and open search modes. The averages are taken over 10 applications, one for each of the 10 target-decoy database pairs we generated for each of the PRIDE-20 dataset.

E.4 Result-related figures

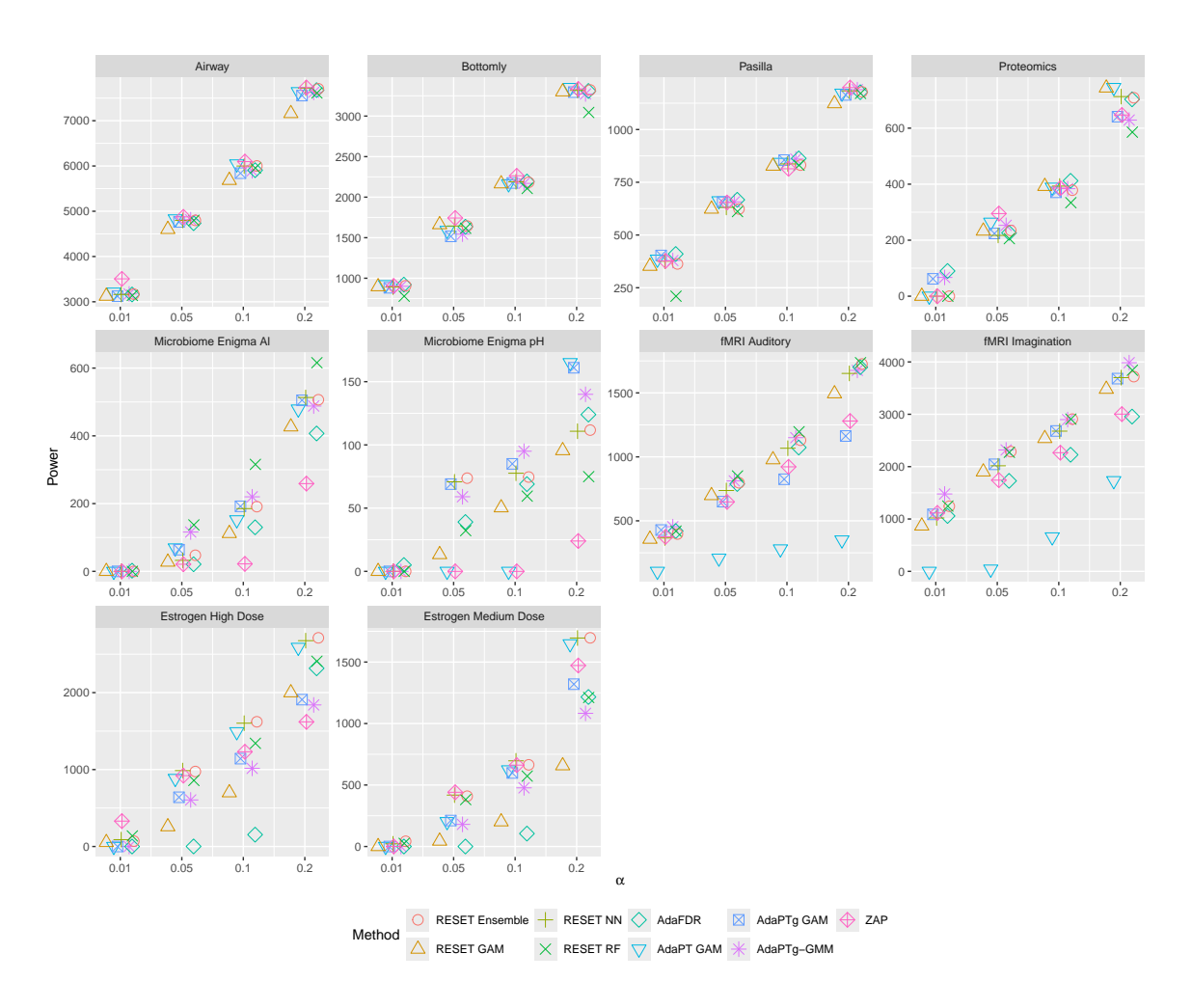


Figure E6: Comparison of RESET and other methods using a collection of publicly available datasets. Each method was evaluated at the FDR thresholds of 1%, 5%, 10%, and 20%. The number of discoveries reported by each RESET method is averaged over 10 applications at FDR threshold and dataset. Each colour and shape combination corresponds to a unique method. For readability, each point is jittered in the horizontal direction.

F Supplementary analyses

F.1 Analysis of AdaDetect and empirical p-values

The main assumption of AdaDetect's FDR control in the novelty detection problem, is that the null observations (Y_1, \ldots, Y_n) and the null test set $(X_i : X_i \sim P_0)$ are exchangeable conditioned on the novelties $(X_i : X_i \not\sim P_0)$ (Marandon et al. (2024)). In the multiple testing setup, the closest analogue to the null observations is the collection of decoy information $\{(\mathbf{x}_i, W_i) : L_i = -1\}$, and the analogue to the null test set is the true null target information $\{(\mathbf{x}_i, W_i) : L_i = 1, i \in N\}$. However the exchangeability assumption of AdaDetect in this setting fails for two reasons: (1) the collection of decoy information $\{(W_i, \mathbf{x}_i) : L_i = -1\}$ contains a mixture of true and false null hypotheses which cannot be discerned and (2) the true null hypotheses can be heterogeneous.

Despite failing to meet the assumptions for guaranteed FDR control, we nonetheless verified this in practice through the following simulation inspired by Zhang et al. (2019). We generated m = 20K hypotheses with side information $\mathbf{x}_i \sim U[0,1]$, each drawn independently. Each hypothesis is declared a false null with probability π_i and a true null otherwise, where

$$\pi_i = \pi(\mathbf{x}_i) := 0.1 \cdot \varphi_{[0.75, 0.05]}^c(\mathbf{x}_i),$$

and $\varphi^c_{[\mu,\sigma]}$ denotes the 0-1 clamping (truncating between 0 and 1) of the normal density with mean μ and standard deviation σ . For each hypothesis we drew $z_i \sim \mathcal{N}(\mu_i, 1)$ where

$$\mu_i = \begin{cases} 3, & \text{if } H_i \text{ is a false null,} \\ 0, & \text{if } H_i \text{ is a true null and } \mathbf{x}_i > 0.25, \\ B_i, & \text{if } H_i \text{ is a true null and } \mathbf{x}_i \leq 0.25, \end{cases}$$

where $B_i \in \{0, -0.5\}$ with equal probability and independent of everything else. One sided p-values are then constructed as $p_i = 1 - \Phi(z_i)$, where Φ is the standard normal CDF. This construction allows us to create a heterogeneous mixture of true nulls that violate the exchangeability assumptions.

We evaluated two versions of RESET on the simulated data, the first is the standard RESET Ensemble as described in Section 4.4 in the main text, and the second adopts AdaDetect's empirical p-value approach, which we now describe. For each target $(L_j = 1)$, we defined the empirical p-value by comparing the target's score with the scores of the estimating decoys:

$$p_j := \frac{1 + \#\{k : \widetilde{W}_k > \widetilde{W}_j, \widetilde{L}_k = +1, L_k = -1\}}{1 + \ell},$$
(8)

where $\ell := \#\{k : \tilde{L}_k = +1, L_k = -1\}$ is the number of estimating decoys. Next, we used Storey's procedure which estimates the fraction of true null hypotheses, π_0 , and applies the BH procedure at the adjusted level of $\alpha/\hat{\pi}_0^{Storey}$. Storey's estimate is given by

$$\hat{\pi}_0^{Storey} := \frac{1 + H(\lambda)}{(1 - \lambda) \cdot \#\{L_k = +1\}},$$

where $H(\lambda)$ denotes the number of empirical p-values $\geq \lambda$. We used $\lambda = \frac{\lfloor \ell/2 \rfloor}{\ell+1}$. This empirical p-value version of RESET is essentially applying the AdaDetect methodology. The only difference is that we can conduct a fair comparison in which both versions of RESET offer the same semi-supervised learning approach.

Figure F1 shows the empirical FDRs using the empirical p-value version of RESET Ensemble (denoted as RESET Ensemble-p) versus the usual RESET Ensemble, averaged over 100 realizations of the data. At 10% and 20% FDR thresholds, we find that empirical FDRs calculated for RESET Ensemble-p are at least 5 standard errors above their respective thresholds, empirically demonstrating failure to control the FDR. Emery et al. (2020) show a similar failure to control the FDR using BH or Storey's procedure using pooled empirical p-values when the true null hypotheses are heterogenous (which they call "noncalibrated").

F.2 Brief justification of the assumptions used with HEK293 and PRIDE-20 datasets

TDC (equivalently SSS+) has become the *de facto* method of FDR analysis in the proteomics literature since its introduction by Elias and Gygi (2007). An assumption of TDC for valid FDR

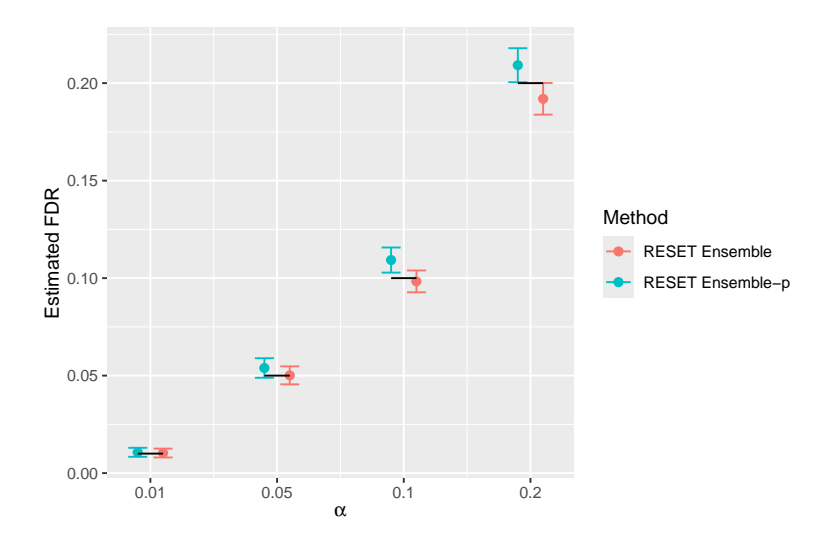


Figure F1: Estimated FDRs with and without empirical p-values. The confidence intervals correspond to ± 5 times the estimated standard error. For readability, points are jittered in the horizontal section. The horizontal segments mark the FDR thresholds on the y-axis.

control is that the label L_i , indicating whether an incorrect target or its decoy scored higher, is uniformly ± 1 independently of all the scores as well as of the labels corresponding to the correct targets (Assumption 1 of the main text). This assumption relies heavily on the decoy construction which we now outline.

There are two main approaches to decoy construction: randomly shuffling or reversing each target peptide sequence. This random shuffling or reversing is typically applied to the non-terminal amino acids, i.e., the amino acids between the first and last. The rationale is that the terminal amino acids of target peptides are typically of a certain type, e.g., lysine or arginine, and therefore they can be used to distinguish target and decoy peptides if they are not preserved. By either shuffling or reversing in this way, the result is a set of decoy peptides that have the exact same length, amino acid profile, and terminal amino acids as their corresponding target peptides, thus creating realistic competition for incorrect target discoveries in an attempt to satisfy the above assumption. While both approaches are commonly used, in this paper we use randomly shuffled decoys so that our results can be averaged across different decoy generations.

Importantly, the above assumption has been corroborated empirically through entrapment experiments (Granholm et al. (2011)). In these experiments, a sample of known peptides is used so that the actual FDP can be gauged. This strategy has allowed others (He et al. (2015); Lin et al. (2022)) to show that the FDR is controlled using TDC, suggesting that Assumption 1 are reasonable in practice.

RESET additionally requires this statement to be true if we further condition on the side information \mathbf{x} . This is obviously true for side information variables that are constant between the target and corresponding decoys — e.g., PepLen, Charge, lnNumSP, dm, absdM. The other side information variables are score-related — e.g., Xcorr, deltCn and deltLCn, and so conditioning on them assumes no more than the 'standard assumption' that already conditions on such a score in the first place. Hence, we believe Assumption 3 with $P(L_i = 1) = c_0 = 1/2$ to be reasonably satisfied. Moreover, in our recent publication, we empirically demonstrated through entrapment experiments that RESET (combined with Percolator, a semi-supervised algorithm designed for peptide detection) controls the FDR (Freestone et al. (2025)).

F.3 Analysis of Adipose datasets

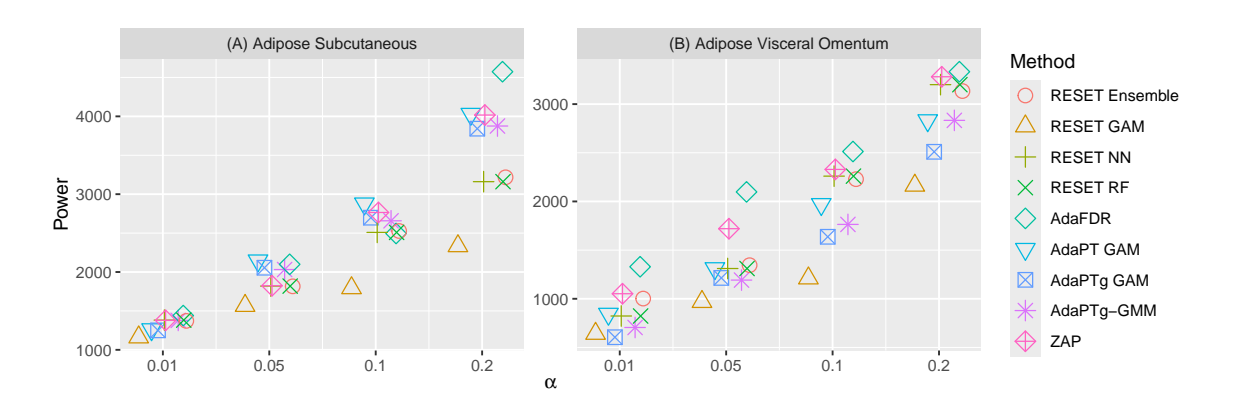


Figure F2: Comparison of power in Adipose data. In (A) and (B), we compare the number of discoveries using the two eQTL datasets. The number of discoveries reported by each RESET method is averaged over 10 applications at a given FDR threshold and dataset. In both panels, we evaluated each method at FDR thresholds of: 1%, 5%, 10%, 20%.

Notably, we have excluded from Figure 6 the analysis of the two eQTL studies for the following reason. Due to linkage disequilibrium these datasets exhibit a high degree of p-value as well as side-information dependency, even among the true null hypotheses. Hence these datasets violate Assumption 3 which guarantees our — as well as the other considered methods' — type-1 error control. It is thus unclear whether our comparisons would remain fair, particularly if one method violates FDR control more than the others. Notably, RESET Ensemble flagged this data as exhibiting suspicious dependence using the feature outlined in Section C.2.4.

Figure F2(A-B) shows that overall RESET Ensemble is able to report a similar number of discoveries to other methods, with the exception of $\alpha = 20\%$ in the Adipose Subcutaneous dataset, where RESET Ensemble reports substantially less discoveries. Even if we overlook the dependency in the data, and include the two eQTL studies in our power analysis in Figure 6, RESET Ensemble still ranks the highest. Indeed, Figure F3 shows the analogous results with the eQTL studies included. RESET Ensemble has the highest median at 93.6%, followed by AdaFDR at 93.2% and RESET NN at 91.8%.

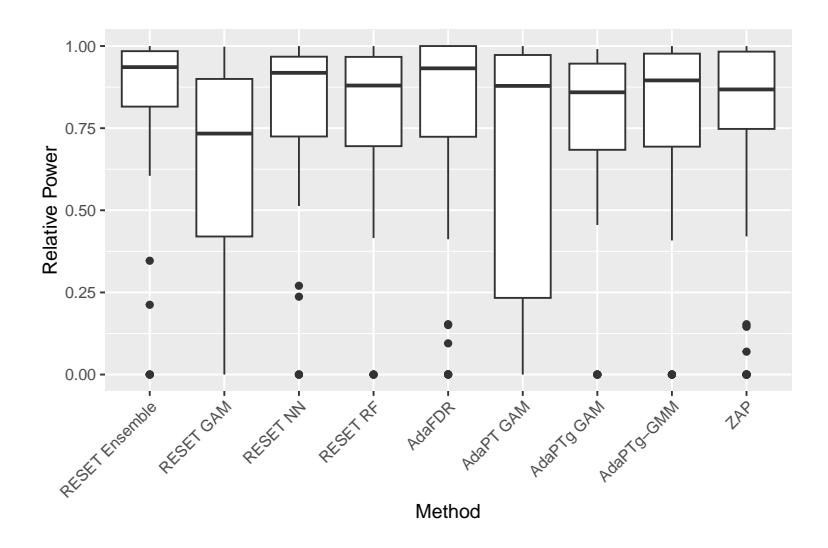


Figure F3: Relative power of each method. The boxplots show the relative power of each method, calculated for each dataset described in Section D.3 (including the two Adipose datasets) and across FDR thresholds of 1%, 5%, 10% and 20%.

F.4 Further analysis of RESET with FDX control

We point out the following limitation on the topic of RESET's FDX control. When the number of discoveries is small, e.g., when the confidence is too high, RESET may yield less power, even if the side information is reasonably informative. To illustrate this phenomenon, we computed the bounds, δ_i on the number of decoy wins in the top i scores from Algorithm A2, which are used to determine the reported list of discoveries in FDP-SD (with c = 1/2) and RESET (using the default c = 2/3). We considered a confidence level of $1 - \gamma = 90\%$ and an FDP threshold of $\alpha = 1\%$. Since we removed approximately half the decoys for training purposes in RESET, the bounds need to be doubled to fairly compare between the two approaches.

Figure F4 shows the bounds for FDP-SD, and double the bounds for RESET, along with the

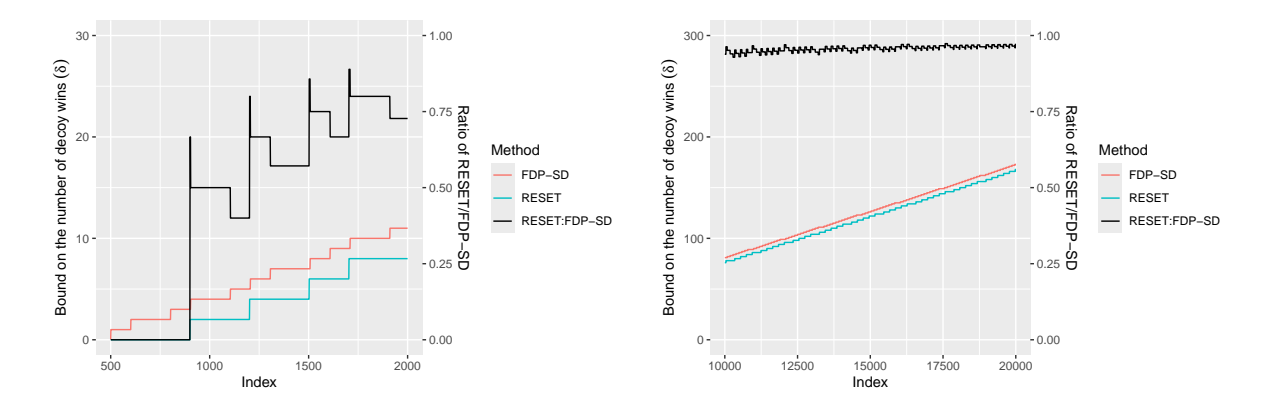


Figure F4: **RESET's and FDP-SD's bounds on the number of decoy wins.** We recorded, on the left y-axis, the bounds used to determine the list of FDP-SD discoveries and twice the bounds used to determine RESET's discoveries at a range of indices at $\alpha = 1\%$ and $1 - \gamma = 90\%$. On the right y-axis, we plot the ratio of these bounds (in black). The left panel looks at indices between 501 to 2K, while the right panel looks at indices from 10K to 20K. An index corresponds to the number of top scoring hypotheses (regardless of their labels).

ratio of the two at a range of different indices. We can see that for smaller indices, this ratio is much smaller, initially at 0% at an index of 501 and 50% at an index of 1K, while at 10K this ratio is much higher at 94%. If the order of the hypotheses is the same, then RESET's smaller bounds imply it will report fewer discoveries because RESET employs FDP-SD to control the FDX by searching for the largest index i s.t. $A_{i_0} \leq \delta_{i_0}, \ldots, A_i \leq \delta_i$, and reports the top i scoring positively labeled hypotheses. In other words, if RESET is to report roughly the same number of discoveries as FDP-SD, then RESET needs to rearrange the targets and estimating decoys successfully enough so as to make up for a 50% difference in the bounds when considering the top 1K scores, while only 6% when considering the top 10K. If the side information is not rich enough, then it is possible RESET will report fewer discoveries than FDP-SD in these cases. We intend to investigate this as part of future work.

F.5 Variability of RESET

RESET's discovery list is variable due to the random split of the decoys. This variability is demonstrated in the histogram of the number of discoveries in Figure F5A using 100 applications of RESET Ensemble to the Airway dataset at an FDR threshold of 10%. The resulting number of discoveries has a mean of 6018 with a standard deviation of about 75.

While this is undesirable, this analysis does not take into account the randomness of the data, and therefore that the added variance from RESET may be marginal. Indeed, in Figure F5B, we find that in the case of Simulation 5 from Section 6.2.1, RESET is overall arguably less variable than AdaPT, even though AdaPT does not employ any internal randomization. In practice, users may get around RESET's randomization by setting the random number generator to be a function of the input data and parameters. We plan on adding this feature to a future update.

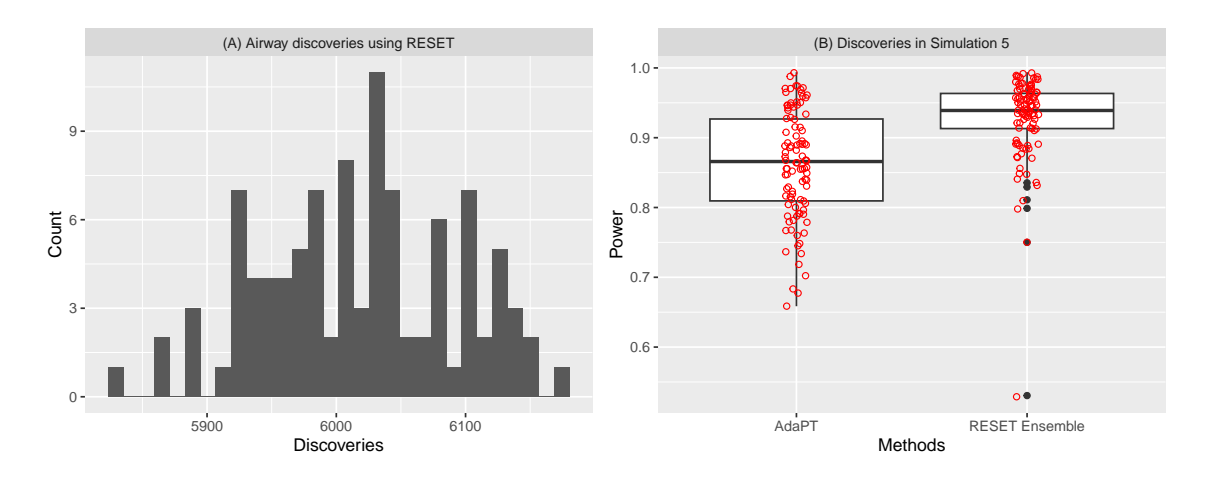


Figure F5: Variability in the number of discoveries. (A) Histogram of the number of RESET Ensemble discoveries applied 100 times to the Airway data with a 10% FDR threshold and varying its internal seed. (B) Boxplots of RESET's and AdaPT's power in 100 applications of the 'circle in the middle' setup of Simulation 5 using a 10% FDR threshold. There is one major outlier in RESET's case (which occurred when the signal was considerably low).